J|A|C|S
ARTICLES

Published on Web 04/16/2008

Palladium Vacataporphyrin Reveals Conformational Rearrangements Involving Hückel and Möbius Macrocyclic Topologies

Ewa Pacholska-Dudziak, Janusz Skonieczny, Miłosz Pawlicki, Ludmiła Szterenberg, Zbigniew Ciunik, and Lechosław Latos-Grażyński*

Department of Chemistry, University of Wrocław, Joliot-Curie 14, 50 383 Wrocław, Poland

Received December 12, 2007; E-mail: llg@wchuwr.pl

Abstract: 5,10,15,20-Tetraaryl-21-vacataporphyrin (butadieneporphyrin, an annulene-porphyrin hybrid) which contains a vacant space instead of heteroatomic bridge acts as a ligand toward palladium(II). The metal ion of square-planar coordination geometry is firmly held via three pyrrolic nitrogen atoms where the fourth coordination place is occupied by a monodentate ligand or by an annulene part of vacataporphyrin. The macrocycle reveals the unique structural flexibility triggered by coordination of palladium. The structural rearrangements engage the C(20)C(1)C(2)C(3)C(4)C(5) annulene fragment which serves as a linker between two pyrrolic rings of vacataporphyrin albeit the significant ruffling of the tripyrrolic block is also of importance. Two fundamental modes of interactions between the palladium ion and annulene moiety have been recognized. The first one resembles an η^2-type interaction and involves the C(2)C(3) unit of the butadiene part. Alternatively the profound conformational adjustments allowed an in-plane coordination through the deprotonated trigonally hybridized C(2) center of butadiene. The coordinated vacataporphyrin acquires Hückel or extremely rare Möbius topologies readily reflected by spectroscopic properties. The palladium vacataporphyrin complexes reveal Hückel aromaticity or Möbius antiaromaticity of [18]annulene applying the butadiene fragment of vacataporphyrin as a topology selector. The properties of specific conformers were determined using ^{1}H NMR and density functional theory calculations.

Introduction

An aza-deficient porphyrin 5,10,15,20-tetraaryl-21-vacataporphyrin (butadieneporphyrin), (VPH_2-*1*)H can be classified as an annulene-porphyrin hybrid (Chart 1).[1,2] In more general terms vacataporphyrin is a representative example of the subclass of modified porphyrins described by a general formula [*n*]triphyrin(*n*.1.1) (n = 1,2, ...).[3–6]

Such a molecule provides the fundamental structural and spectroscopic features of parental 5,10,15,20-tetraarylporphyrin.[1] Actually this macrocycle has an expanded coordination core, comparable by size and shape with texaphyrin,[7,8] and related to theoretically investigated secophyrin.[9] As illustrated by comparison to texaphyrin[10–12] the annulene fragment of vacataporphyrin is suitably exposed to coordination or interaction with initially nitrogen-coordinated metal ions. Consequently vacata-

Chart 1. Vacataporphyrin, (VPH_2-1)H, Ar = 4-Metoxyphenyl (Anis), *p*-Tol

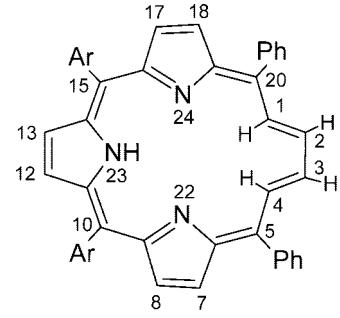

(VPH_2-1)H

(1) Pacholska, E.; Latos-Grażyński, L.; Ciunik, Z. *Chem. Eur. J.* **2002**, *8*, 5403–5406.
(2) From now on we will use the symbol (VPH_2-*n*) to denote the hypothetical monoanion obtained from the vacataporphyrin by abstraction of a pyrrolic NH proton. The hypothetical dianion formed by abstraction the C-bound proton H(2) is noted as (VPH-*n*). The group attached to C(2/3) will appear as a suffix. Finally the appropriate macrocyclic conformers are systematically numbered (n) as occur in the text. The neutral structure is described by the following acronym (VPH_2-*n*)H.
(3) Franck, B.; Nonn, A. *Angew. Chem., Int. Ed. Engl.* **1995**, *34*, 1795–1811.
(4) Krivokapic, A.; Cowley, A. R.; Anderson, H. L. *J. Org. Chem.* **2003**, *68*, 1089–1096.
(5) Inokuma, Y.; Kwon, J. H.; Ahn, T. K.; Yoo, M.-C.; Kim, D.; Osuka, A. *Angew. Chem., Int. Ed.* **2006**, *45*, 961–964.
(6) Kobayashi, N.; Takeuchi, Y.; Matsuda, A. *Angew. Chem., Int. Ed.* **2007**, *46*, 758–760.
(7) Sessler, J. L.; Murai, T.; Lynch, V.; Cyr, M. *J. Am. Chem. Soc.* **1988**, *110*, 5586–5588.
(8) Hannah, S.; Lynch, V. M.; Gerasimchuk, N.; Magda, D.; Sessler, J. L. *Org. Lett.* **2001**, *3*, 3911–3914.
(9) Waluk, J.; Michl, J. *J. Org. Chem.* **1991**, *56*, 2729–2745.
(10) Sessler, J. L.; Hemmi, G.; Mody, T. D.; Murai, T.; Burrell, A.; Young, S. W. *Acc. Chem. Res.* **1994**, *27*, 43–50.
(11) Lisowski, J.; Sessler, J. L.; Lynch, V.; Mody, T. D. *J. Am. Chem. Soc.* **1995**, *117*, 2273–2285.
(12) Hannah, S.; Lynch, V.; Guldi, D. M.; Gerasimchuk, N.; MacDonald, C. L. B.; Magda, D.; Sessler, J. L. *J. Am. Chem. Soc.* **2002**, *124*, 8416–8427.

10.1021/ja711039c CCC: $40.75

Chart 2. Stereoisomers of (VPH_2-*n*)M^{II}Cl (M = Zn, Cd, Ni)

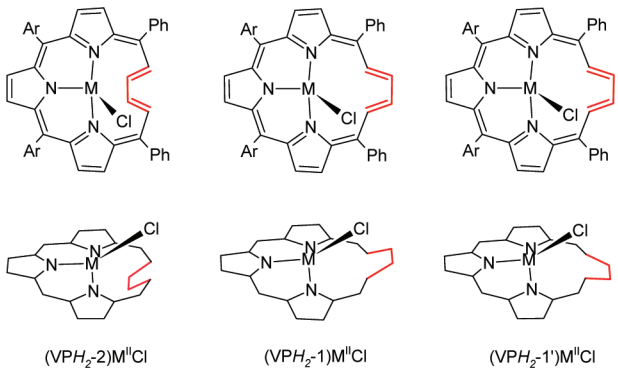

porphyrin may eventually reveal its carbaporphyrinoid nature. In general carbaporphyrinoids provide a unique macrocyclic platform which is suitable to explore organometallic chemistry confined to a peculiar macrocyclic environment.[13–18] Such an entrapment enforces frequently an unusual coordination geometry involving M···(H−C), M···$(CH)_2$ or M−C fragments.

As we have previously demonstrated vacataporphyrin forms diamagnetic (VPH_2)Zn^{II}Cl and (VPH_2)Cd^{II}Cl and paramagnetic (VPH_2)Ni^{II}Cl complexes.[19] A metal ion is bound in the macrocyclic cavity by three pyrrolic nitrogens. Coordination imposes a steric constraint on ligand geometry and leads to stereoisomers with the annulene part oriented outward (VPH_2-1)M^{II}Cl or toward (VPH_2-2)M^{II}Cl the macrocyclic center (Chart 2). The (VPH_2-1)Cd^{II}Cl, (VPH_2-1)Zn^{II}Cl complexes and the free base (VPH_2-1)H share a common ^{1}H NMR spectral pattern as the basic structural features are preserved after metal ion insertion. The ^{1}H NMR spectra of (VPH_2-2)Cd^{II}Cl and (VPH_2-2)Zn^{II}Cl reflect a considerable decrease of aromaticity accounted by inverted geometry. The annulene-metal ion proximity induces direct couplings between the spin-active nucleus of the metal ($^{111/113}$Cd) and the adjacent ^{1}H nuclei of annulene.

To explore coordinating properties of vacataporphyrin here we have focused on coordination chemistry of palladium. A variety of palladium(II) complexes with porphyrins,[20] expanded porphyrins,[21] heteroporphyrins,[22] and carbaporphyrins[23–29] have been isolated and characterized. Importantly, the palladium(II) ion is susceptible to phenyl coordination in a cyclopalladation process.[30–32] Once the carbon donor is built into macrocylic[33] or pincer ligands the palladium(II) ion forms robust organometallic compounds.[30,33–36] Markedly a peculiar coordination mode has been detected for a Pd_2^{2+} couple sandwiched between two helical bilindione-palladium moieties. The compound reveals η^2-coordination of a palladium center to the π system at one of the $C_{meso}-C_\alpha$ bonds.[37]

In the course of our present investigations we have realized that coordination of palladium(II) to three pyrrolic nitrogens of vacataporphyrins triggers a spectacular sequence of conformational changes, which have been readily visualized by ^{1}H NMR spectroscopy as the respective spectra reflect distinct diatropic or moderate paratropic effects. These spectroscopic features made us receptive to the [18]annulene model of a porphyrin,[38] which, emphasizing the presence of an 18-electron main π-conjugation pathway in the molecule, invites the application of Hückel rule to the tetrapyrrolic macrocycle. In ^{1}H NMR spectroscopic terms this electronic feature is typically reflected by a well-defined diatropic effect detectable even for the most severe distortion of [18]porphyrins(1.1.1.1).[39] Significantly such an effect has been detected even for folded porphyrin derivatives of C_s symmetry: 21,23-ditelluraporphyrin which contains a single flipped tellurophene ring,[40] nonplanar *p*-benziporphyrin,[16,41–43] and vacataporphyrin complexes containing inverted butadiene fragment.[19]

Extending the [18]annulene model of porphyrin, in direct analogy to [*n*]annulenes we have put forward a hypothesis that twisted vacataporphyrin may acquire Hückel aromaticity or Möbius antiaromaticity.[44,45] The special energetics of π-systems for Möbius annulenes was first considered over 40 years ago.[46] The flexible systems, such as higher annulenes, prefer to adopt untwisted Hückel topologies, which are normally more stable.[44,47,48] While computational data indicate that Möbius conformations might contribute to chemistry of higher [4*n*]annulenes,[49,50] so far they have not been identified experimentally.

(13) Harvey, J. D.; Ziegler, C. J. *Coord. Chem. Rev.* **2003**, *247*, 1–19.
(14) Srinivasan, A.; Furuta, H. *Acc. Chem. Res.* **2005**, *38*, 10–20.
(15) Chmielewski, P. J.; Latos-Grażyński, L. *Coord. Chem. Rev.* **2005**, *249*, 2510–2533.
(16) Stępień, M.; Latos-Grażyński, L. *Acc. Chem. Res.* **2005**, *38*, 88–98.
(17) Maeda, H.; Furuta, H. *Pure Appl. Chem.* **2006**, *78*, 29–44.
(18) Pawlicki, M.; Latos-Grażyński, L. *Chem. Rec.* **2006**, *6*, 64–78.
(19) Pacholska-Dudziak, E.; Skonieczny, J.; Pawlicki, M.; Latos-Grażyński, L.; Szterenberg, L. *Inorg. Chem.* **2005**, *44*, 8794–8803.
(20) Stolzenberg, A. M.; Schussel, L.; Summers, J. S.; Foxman, B. M.; Petersen, J. L. *Inorg. Chem.* **1992**, *31*, 1678–1686.
(21) Shimizu, S.; Osuka, A. *Eur. J. Inorg. Chem.* **2006**, 1319–1335.
(22) Latos-Grażyński, L.; Lisowski, J.; Chmielewski, P. J.; Grzeszczuk, M.; Olmstead, M. M.; Balch, A. L. *Inorg. Chem.* **1994**, *33*, 192–197.
(23) Stępień, M.; Latos-Grażyński, L.; Lash, T. D.; Szterenberg, L. *Inorg. Chem.* **2001**, *40*, 6892–6900.
(24) Pawlicki, M.; Latos-Grazyński, L. *Chem. Eur. J.* **2003**, *9*, 4650–4660.
(25) Stępień, M.; Latos-Grażyński, L. *Chem. Eur. J.* **2001**, *7*, 5113–5117.
(26) Lash, T. D.; Colby, D. A.; Graham, S. R.; Ferrence, G. M.; Szczepura, L. F. *Inorg. Chem.* **2003**, *42*, 7326–7338.
(27) Liu, D.; Lash, T. D. *Chem. Commun.* **2002**, 2426–2427.
(28) Venkatraman, S.; Anand, V. G.; Pushpan, S. K.; Sankar, J.; Chandrashekar, T. K. *Chem. Commun.* **2002**, 462–463.
(29) Furuta, H.; Maeda, H.; Osuka, A.; Yasutake, M.; Shinmyozu, T.; Ishikawa, Y. *Chem. Commun.* **2000**, 1143–1144.
(30) Steenwinkel, P.; Gossage, R. A.; van Koten, G. *Chem. Eur. J.* **1998**, *4*, 759–762.
(31) Steenwinkel, P.; Gossage, R. A.; Maunula, T.; Grove, D. M.; van Koten, G. *Chem. Eur. J.* **1998**, *4*, 763–768.
(32) Jolliet, P.; Gianini, M.; von Zelewsky, A.; Bernardinelli, G.; Stoeckli-Evans, H. *Inorg. Chem.* **1996**, *35*, 4883–4888.
(33) Giesbrecht, G. R.; Hanan, G. S.; Kickham, J. E.; Loeb, S. J. *Inorg. Chem.* **1992**, *31*, 3286–3291.
(34) Rietveld, M. H. P.; Grove, D. M.; van Koten, G. *New J. Chem.* **1997**, *21*, 751–771.
(35) van Koten, G. *Pure Appl. Chem.* **1989**, *61*, 1681–1694.
(36) van der Boom, M. E.; Liou, S. Y.; Ben David, Y.; Shimon, L. J. W.; Milstein, D. *J. Am. Chem. Soc.* **1998**, *120*, 6531–6541.
(37) Lord, P.; Olmstead, M. M.; Balch, A. L. *Angew. Chem., Int. Ed.* **1999**, *38*, 2761–2763.
(38) Vogel, E. *Pure Appl. Chem.* **1993**, *65*, 143–152.
(39) Medforth, C. J. NMR Spectroscopy of Diamagnetic Porphyrins. In *The Porphyrin Handbook*; Kadish, K. M., Smith, K. M., Guilard, R., Eds.; Academic Press: San Diego, CA, 2000; pp 1−80.
(40) Pacholska, E.; Latos-Grażyński, L.; Ciunik, Z. *Angew. Chem., Int. Ed.* **2001**, *40*, 4466–4469.
(41) Stępień, M.; Latos-Grażyński, L. *J. Am. Chem. Soc.* **2002**, *124*, 3838–3839.
(42) Stępień, M.; Latos-Grażyński, L.; Szterenberg, L.; Panek, J.; Latajka, Z. *J. Am. Chem. Soc.* **2004**, *126*, 4566–4580.
(43) Stępień, M.; Latos-Grażyński, L.; Szterenberg, L. *Inorg. Chem.* **2004**, *43*, 6654–6662.
(44) Rzepa, H. S. *Chem. Rev.* **2005**, *105*, 3697–3715.
(45) Warner, P. M. *J. Org. Chem.* **2006**, *71*, 9271–9282.
(46) Heilbronner, E. *Tetrahedron Lett.* **1964**, *5*, 1923–1928.
(47) Herges, R. *Chem. Rev.* **2006**, *106*, 4820–4842.
(48) Castro, C.; Isborn, C. M.; Karney, W. L.; Mauksch, M.; Schleyer, P. *Org. Lett.* **2002**, *4*, 3431–3434.

The Möbius π-systems were proposed as transition states[49–52] and reactive intermediates.[53] The first examples of stable, neutral Möbius π systems, that is, biantraquinodimethane modified [16]annulenes, have been synthesized only recently by Herges and co-workers.[54,55] In those molecules, the twist was achieved by combining normal and in-plane conjugation. The effect of benzannelation on Möbius [4*n*]annulene aromaticity in these compounds was analyzed by Schleyer and co-workers.[56] Recently we have presented the first example of dynamic switching between Hückel and Möbius topologies in a conjugated molecule. This effect is documented for an expanded porphyrin analogue containing para-phenylene rings A,D-di-*p*-benzi[28]hexaphyrin.[57] Subsequently Osuka and co-workers demonstrated that Möbius aromatic molecules are spontaneously formed upon metalation of meso-aryl-substituted expanded porphyrins ([36]octaphyrin, [32]heptaphyrin, [26]heptaphyrin, and N-fused [24]pentaphyrin).[58,59]

The present contribution describes the synthesis and properties of palladium vacataporphyrin complexes which reveal Hückel aromaticity or Möbius antiaromaticity of [18]annulene applying a butadiene fragment of vacataporphyrin as a topology selector. Their behavior was studied using spectroscopic and computational methods.

Results and Discussion

Formation and Characterization of (VP*H*$_2$-1)Pd^{II}Cl. Reaction of $Pd(PhCN)_2Cl_2$ with vacataporphyrin, (VP*H*$_2$-1)H in chloroform results in the formation of the four-coordinate (VP*H*$_2$-1)Pd^{II}Cl (Scheme 1).

Scheme 1. Synthesis of (VP*H*$_2$-1)Pd^{II}Cl. Ar = 4-Metoxyphenyl (Anis), *p*-Tol

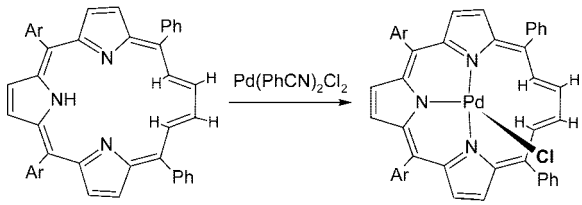

(VP*H*$_2$-1)H (VP*H*$_2$-1)Pd^{II}Cl

To obtain a single well-defined product it is absolutely necessary to carry out the insertion in the dark. It has been also found that (VP*H*$_2$-1)Pd^{II}Cl undergoes demetalation in acidic solutions.

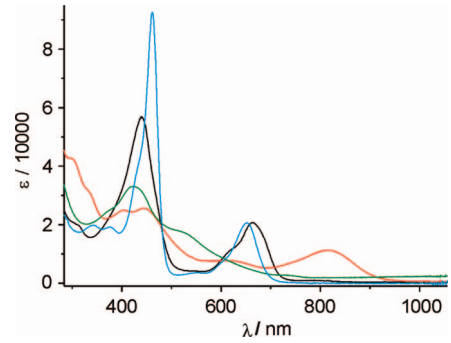

Figure 1. The electronic spectra of (VP*H*$_2$-1)Pd^{II}Cl (black line), (VP*H*-3)Pd^{II} (blue line), [(VP*H*$_2$-4)Pd^{II}]BF_4 (green line), and [(VP*H*$_2$-5)Pd^{II}]BF_4 (red line) in CH_2Cl_2.

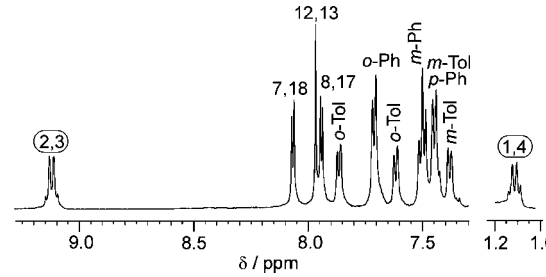

Figure 2. ^{1}H NMR spectrum of (VP*H*$_2$-1)Pd^{II}Cl, Ar = *p*-Tol ($CDCl_3$, 298 K).

The vacataporphyrin acts as a monoanionic ligand coordinating through the three nitrogen donors. To complete the coordination sphere of metal dication one additional ligand is required. Originally the identity of (VP*H*$_2$-1)Pd^{II}Cl was confirmed by high resolution mass spectrometry and NMR spectroscopy. The electronic absorption spectrum of (VP*H*$_2$-1)Pd^{II}Cl is shown in Figure 1 (solid black line). A porphyrin-like pattern is clearly present with a distinct Soret-like band (440 nm) and a set of bands in the Q region. The spectral pattern resembles that of (VP*H*$_2$-1)Cd^{II}Cl and (VP*H*$_2$-1)Zn^{II}Cl providing that the reference spectra were collected under conditions where the (VP*H*$_2$-1)M^{II}Cl stereoisomer prevailed in solution.[19]

(VP*H*$_2$-1)Pd^{II}Cl has an effective C_s symmetry, with the mirror plane passing through the metal ion, chloride, and pyrrolic N(23) nitrogen. As a consequence, the ^{1}H NMR spectrum (Figure 2) contains three pyrrole resonances (H(7)/H(18), H(8)/H(17), and H(12)/H(13)) and two multiplets of butadiene resonances (H(1)/H(4) and H(2)/H(3)). Nonequivalence of two macrocyclic sides causes each aryl ring to have two distinct ortho and two meta resonances, unless the rotation around the $C_{meso}-C_{ipso}$ bond is sufficiently fast. The (VP*H*$_2$-1)Pd^{II}Cl stereoisomer has been unambiguously identified as a single product of insertion in the dark (Scheme 1). Thus (VP*H*$_2$-1)Pd^{II}Cl shares a common ^{1}H NMR spectral pattern with the free base or (VP*H*$_2$-1)Cd^{II}Cl.[19] In particular the AA′XX′ multiplets are consistent with an extended structure of C(1)C(2)C(3)C(4) annulene moiety (Figure 2, Scheme 1). Actually the determined ^{1}H NMR parameters closely resemble those of [18]annulene.[60] On the other hand ^{1}H NMR spectrum of the pyrrolic part of (VP*H*$_2$-1)Pd^{II}Cl exhibits values of *J* and δ which are typical for tetraaryl-21-

(49) Castro, C.; Karney, W. L.; Valencia, M. A.; Vu, C. M. H.; Pemberton, R. P. *J. Am. Chem. Soc.* **2005**, *127*, 9704–9705.
(50) Pemberton, R. P.; McShane, C. M.; Castro, C.; Karney, W. L. *J. Am. Chem. Soc.* **2006**, *128*, 16692–16700.
(51) Zimmerman, H. E. *J. Am. Chem. Soc.* **1966**, *88*, 1564–1565.
(52) Moll, J. F.; Pemberton, R. P.; Gutierrez, M. G.; Castro, C.; Karney, W. L. *J. Am. Chem. Soc.* **2007**, *129*, 274–275.
(53) Mauksch, M.; Gogonea, V.; Jiao, H.; Schleyer, P. v. R. *Angew. Chem., Int. Ed. Engl.* **1998**, *37*, 2395–2398.
(54) Ajami, D.; Oeckler, O.; Simon, A.; Herges, R. *Nature* **2003**, *426*, 819–821.
(55) Ajami, D.; Hess, K.; Köhler, F.; Näther, C.; Oeckler, O.; Simon, A.; Yamamoto, C.; Okamoto, Y.; Herges, R. *Chem. Eur. J.* **2006**, *12*, 5434–5445.
(56) Castro, C.; Chen, Z.; Wannere, C. S.; Jiao, H.; Karney, W. L.; Mauksch, M.; Puchta, R.; Hommes, N. J. R.; Schleyer, P. *J. Am. Chem. Soc.* **2005**, *127*, 2425–2432.
(57) Stępień, M.; Latos-Grażyński, L.; Sprutta, N.; Chwalisz, P.; Szterenberg, L. *Angew. Chem., Int. Ed.* **2007**, *46*, 7869–7874.
(58) Tanaka, Y.; Saito, S.; Mori, S.; Aratani, N.; Shinokubo, H.; Shibata, N.; Higuchi, Y.; Yoon, Z. S.; Kim, K. S.; Noh, S. B.; Park, J. K.; Kim, D.; Osuka, A. *Angew. Chem., Int. Ed.* **2008**, *47*, 693–696.
(59) Park, J. K.; Yoon, Z. S.; Yoon, M.-C.; Kim, K. S.; Mori, S.; Shin, J.-Y.; Osuka, A.; Kim, D. *J. Am. Chem. Soc.* **2008**, *130*, 1824–1825.
(60) Stevenson, C. D.; Kurth, T. L. *J. Am. Chem. Soc.* **2000**, *122*, 722–723.

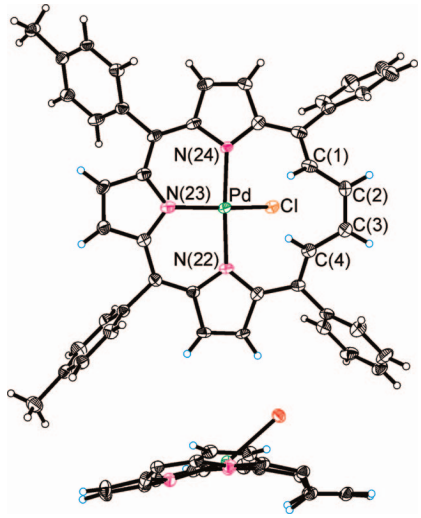

Figure 3. The crystal structure of (VPH_2-1)$Pd^{II}Cl$ (top, perspective view; bottom, side view; phenyl groups omitted for clarity). The thermal ellipsoids represent 50% probability.

Scheme 2. Formation of Palladium(II) Vacataporphyrin Complex Containing the Pd−C Bond, (VP*H*-3)Pd^{II}

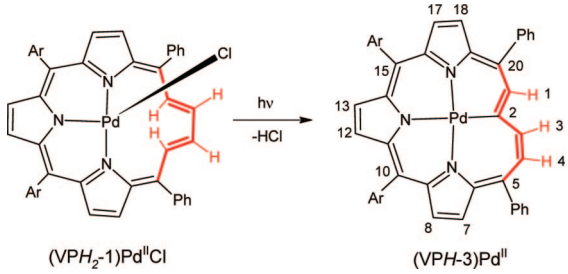

heteroporphyrins.[61] The $\delta_{H(2)} - \delta_{H(1)}$ chemical shift difference equal to 8.01 ppm (for Ar = *p*-Tol, see Scheme 1), considered as the experimental criterion of aromaticity,[62–64] is significantly smaller than the 12.15, 10.77, and 9.28 ppm values determined for (VPH_2-1)H, (VPH_2-1)$Cd^{II}Cl$, and (VPH_2-1)$Zn^{II}Cl$, respectively.[19] The coordination imposes the macrocyclic nonplanarity which is revealed by the diminished ring current.

The structure of (VPH_2-1)$Pd^{II}Cl$ has been determined by X-ray crystallography. Perspective views of the molecule are shown in Figure 3. The geometry of the complex reflects the balance among constraints of the macrocycle ligand, the size of the palladium ion, and the predisposition of the palladium for square planar geometry.

The palladium atom is bound to three nitrogen atoms. The Pd−N bond lengths (Pd−N(23): 2.021(4), Pd−N(24): 2.069(4), Pd−N(22): 2.073(3) Å) fall in the range of distances (2.00−2.08 Å) seen for palladium porphyrins.[20,22,65–67] The annulene fragment is remote from the palladium (Pd···C(1), 3.31; Pd···H(1), 2.89; Pd···C(2), 4.19; Pd···H(2), 5.05 Å). The distinct features of the structure are the planar (approximately) butadiene moiety displaced above the C_{meso} plane (C(5)-C(10)C(15)C(20)) and the very pronounced bending of the chloride ligand toward the annulenic unit. Significantly the N(22)−Pd−N(24) fragment (170.0(1)°) is only slightly distorted from linearity, while N(23)−Pd−C(l) is bent (155.4(1)°) as a consequence of strain induced by incorporation of a metal−chloride bond into a macrocycle with a limited core. The angle between the butadiene plane and the plane of the four meso carbons ($C_{butadiene}/C_{meso}$) is relatively small and equals 3.5°. Actually the nearly parallel position of the $C_{butadiene}$ and C_{meso} planes seen at the Figure 3 (the side-on projection) is nicely reflected by the displacement the C(1), C(2), C(3), C(4) atoms from the C_{meso} plane (C(1) 0.74, C(2) 0.69, C(3) 0.64, C(4) 0.55 Å). The bond distances within the tripyrrolic and annulenic framework of complexes indicate that the macrocycle is highly conjugated following the free base pattern.[1]

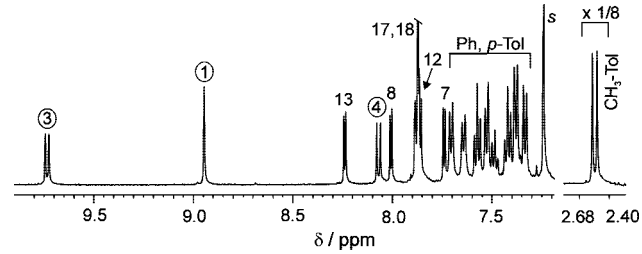

Figure 4. ^{1}H NMR spectrum of (VP*H*-3)Pd^{II}, Ar = *p*-Tol ($CDCl_3$, 298 K). Resonance assignments follow the numbering given in Scheme 2.

Formation and Characterization of (VP*H*-3)Pd^{II}. The photochemical isomerization (VPH_2-1)$M^{II}Cl \rightleftarrows$ (VPH_2-2)$M^{II}Cl$ was previously detected for cadmium(II) and zinc(II) complexes.[19] Initially a sample of (VPH_2-1)$Pd^{II}Cl$ has been exposed to light in an attempt to generate an expected (VPH_2-2)$Pd^{II}Cl$ stereoisomer. The progress of the reaction has been followed by electronic spectroscopy. After one hour the spectrum of (VPH_2-1)$Pd^{II}Cl$ has been completely replaced by a spectrum of aromatic (VP*H*-3)Pd^{II}, differentiated from the original one by batochromic shifts of major bands (Figure 1). In particular the Soret band becomes more intense and shifts batochromically to 461 nm. The reaction proceeds with well-defined isosbestic points proving that the conversion has not included any abundant intermediate form. The novel organopalladium(II) complex (VP*H*-3)Pd^{II} (Scheme 2) results from an intramolecular carbapalladation.

The ^{1}H NMR spectrum of (VP*H*-3)Pd^{II} (Figure 4) differs from that determined till present for any stereoisomer of vacataporphyrin complexes. Specifically the increased multiplicity of resonances indicates the full asymmetry of the acting ligand. The most notable feature of (VP*H*-3)Pd^{II} is coordination of palladium(II) in the plane of the butadiene fragment through the unprotonated trigonally hybridized C(2) center. The H(2) resonance of (VPH_2-1)$Pd^{II}Cl$, located at 9.14 ppm, is absent in the ^{1}H NMR spectrum of (VP*H*-3)Pd^{II}. Consistently the AA′XX′ spin system, H(1)H(2)H(3)H(4), of (VPH_2-1)$Pd^{II}Cl$, has been replaced by the AMX, H(1)H(3)H(4), of (VP*H*-3)Pd^{II}. Importantly the $^3J_{H(3)H(4)}$ coupling constant equals 9.2 Hz and is consistent with the cis geometry of C(2)C(3)C(4)C(5). Partial

(61) Latos-Grażyński, L. Core Modified Heteroanalogues of Porphyrins and Metalloporphyrins. In *The Porphyrin Handbook*; Kadish, K. M., Smith, K. M., Guilard, R., Eds.: Academic Press: New York, 2000; pp 361−416.
(62) Konig, H.; Eickmeier, C.; Moller, M.; Rodewald, U.; Frank, B. *Angew. Chem., Int. Ed. Engl.* **1990**, *29*, 1393–1395.
(63) Chmielewski, P. J.; Latos-Grażyński, L.; Rachlewicz, K. *Chem. Eur. J.* **1995**, *1*, 68–73.
(64) Sprutta, N.; Latos-Grażyński, L. *Chem. Eur. J.* **2001**, *7*, 5099–5112.
(65) Golder, A. J.; Milgrom, L. R.; Nolan, K. E.; Povey, D. C. *Chem. Commun.* **1987**, 1788–1790.
(66) Vogel, E.; Bröring, M.; Erben, C.; Demuth, R.; Lex, J.; Nendel, M.; Houk, K. N. *Angew. Chem., Int. Ed. Engl.* **1997**, *36*, 353–357.
(67) McGhee, E.; Hoffman, B. M.; Ibers, J. A. *Inorg. Chem.* **1991**, *39*, 2162–2165.

Scheme 3. Alkylation and Protonation of (VP*H*-3)Pd^{II}

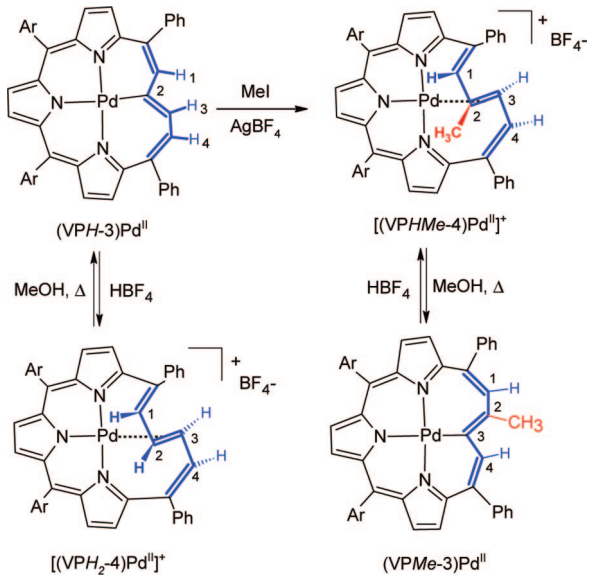

assignments of ^{13}C resonances have been carried out using ^{1}H−^{13}C correlation techniques (HMQC, HMBC). The chemical shift found for C(2) (150.8 ppm) is indicative of the sp^2 hybridization. Thus the NMR data provide an evidence for the coordination of the aromatic dianionic ligand derived from (VPH_2-1)H after the dissociation of NH and C(2)H protons.

Alkylation and Protonation of (VP*H*-3)Pd^{II}. Of particular importance is the observation that (VP*H*-3)Pd^{II} is susceptible to methylation at the C(2) atom. Thus (VP*H*-3)Pd^{II} rapidly reacts with methyl iodide but only in presence of $AgBF_4$ to yield a unique organopalladium(II) complex [(VP*HMe*-4)Pd^{II}]BF_4 (Scheme 3).

Judging by the ^{1}H NMR spectrum of the reaction mixture, the process is nearly quantitative provided that there are no traces of water. The selectively deuterated [(VP*H*(*Me*-d_3)-4)Pd^{II}]$^+$ has been obtained using methyl-d_3 iodide. Protonation causes spectral changes which resemble those resulting from methylation. Thus [(VPH_2-4)Pd^{II}]$^+$ has been generated by addition of HBr in CH_3COOH or HBF_4 in Et_2O to (VP*H*-3)Pd^{II} (Scheme 3, Figure 5). An HBF_4 titration has been carried out in CD_2Cl_2 (200 K) and the progress of this reaction has been monitored by ^{1}H NMR. The feasible palladium-centered hydrogenation to form [(VP*H*-4)Pd^{IV}H]$^+$ has not been detected. The protonation is reversible. Thus heating the solution of [(VPH_2-4)Pd^{II}]$^+$ with addition of methanol recovers (VP*H*-3)Pd^{II} (Scheme 3). The analogous deprotonation of [(VP*HMe*-4)Pd^{II}]$^+$ follows the similar path producing the appropriate C-methylated aromatic derivative (VP*Me*-3)Pd^{II}(Scheme 3).

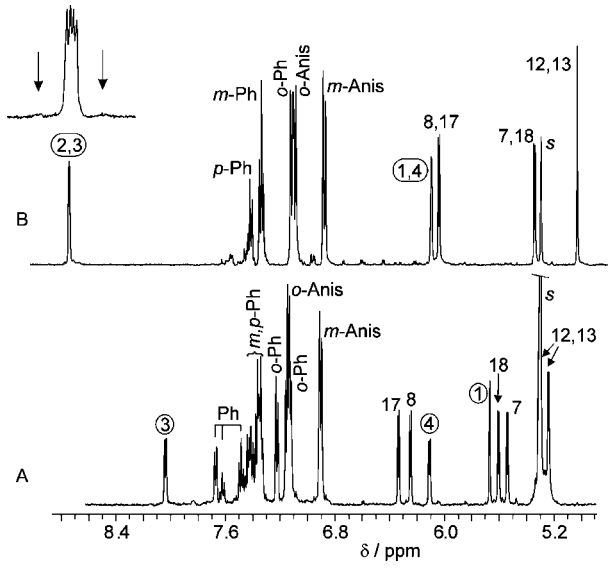

Figure 5. ^{1}H NMR spectra (CD_2Cl_2, 298 K, Ar = Anis) of (A) (VP*HCH*$_3$-4)Pd^{II}, (B) [(VPH_2-4)Pd^{II}]$^+$, Ar = Anis. Resonance assignments follow the numbering given in Scheme 3. Inset presents the details of the H(2,3) multiplet.

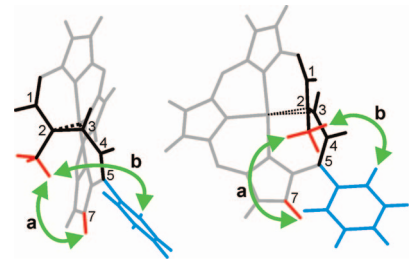

Figure 6. Drawing of the [(VP*HMe*-4)Pd^{II}]$^+$ skeleton as obtained from the DFT (B3LYP) optimization. Meso-aryl rings were omitted for clarity. Arrows indicate the selected contacts, which are crucial in the interpretation of the NOE relays. The distances equal (a) 3.53 Å, (b) 3.67 Å.

The representative ^{1}H NMR spectral patterns of [(VPH_2-4)Pd^{II}]$^+$ and [(VP*HMe*-4)Pd^{II}]$^+$ are shown in Figure 5. The unambiguous assignments of resonances, which are given above selected groups of peaks have been made on the basis of relative intensities and detailed two-dimensional NMR. Importantly the 2D NMR studies have been accompanied by crucial assignments achieved via specific deuterium labeling of vacataporphyrin complexes. The deuterated derivative (VPH_2-d_x)H ($x > 2$), where deuterium atoms are bound to C(1) and C(4) and to some extent to β-pyrrolic carbon atoms, has been synthesized as described previously.[1] The localization and degree of deuteration has been readily determined for (VPH_2-d_x-1)Pd^{II}Cl. The deuteration has resulted in diminished intensity of the H(1) and H(4) resonance(s) for (VPH_2-d_x-1)Pd^{II}Cl and subsequently for each compound generated in the sequence of processes (Scheme 2, 3). The peculiar paratropicity of [(VPH_2-4)Pd^{II}]$^+$ and [(VP*HMe*-4)Pd^{II}]$^+$ is evident from unusual features of their ^{1}H NMR spectra (discussed here for the 10,15-di-(*p*-tolyl) derivative). The β-H signals of both species are shifted upfield relative to nonaromatic fully conjugated systems which contain pyrrole moieties.[25,68] The ^{1}H NMR spectrum of [(VPH_2-4)Pd^{II}]$^+$ exhibits one AB (at 5.89 and 5.33 ppm) and one A_2 (4.95 ppm) patterns assigned to pyrrole protons. The reversed order of meso-aryl resonances has been observed (*p*-H > *m*-H > *o*-H). In particular the upfield relocation of the ortho protons (phenyl 7.15, *p*-tolyl 7.01 ppm) seems to be of significance. In the case of the 10,15-bis(4-methoxyphenyl) derivative, the influence of methoxy substituent obscures the paratropic effect. The peculiar position of the methine H(2), H(3) resonance at 8.98 ppm has also been noted. Significantly, the adjacent H(1) hydrogen produces the resonance at 6.18 ppm. The spectroscopic pattern observed for [(VPH_2-4)Pd^{II}]$^+$ is apparently consistent with a pronounced folding of the macrocyle and palladium η^2-alkene coordination (vide infra) and indicates Möbius antiaromaticity of this $4n+2$ π-electron system.[44,46,47] At the same time

(68) Myśliborski, R.; Latos-Grażyński, L. *Eur. J. Org. Chem.* **2005**, 5039–5048.

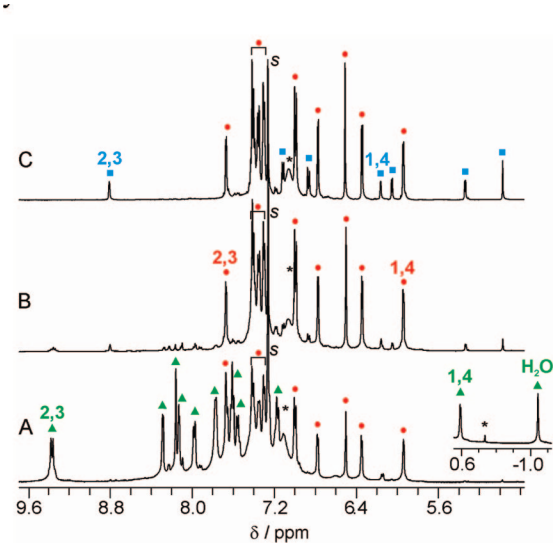

Figure 7. ^{1}H NMR spectra (250 K, $CDCl_3$, Ar = Anis) showing the transformation of $[(VPH_2\text{-}1)Pd^{II}(H_2O)]^+$, prepared from $(VPH_2\text{-}1)Pd^{II}Cl$ and $AgBF_4$ in $CDCl_3$. The mixture held in 298 K for (A) 90 s, (B) 150 s, (C) 2 h; then cooled to 250 K. Labeling: green triangle, $[(VPH_2\text{-}1)Pd^{II}(H_2O)]^+$; red dot, $[(VPH_2\text{-}5)Pd^{II}]^+$; blue square, $[(VPH_2\text{-}4)Pd^{II}]^+$.

the ^{13}C chemical shift of C(2) (100.1 ppm) is consistent with the carbon coordination (the chemical shift for noncoordinated C(1) equals 125.3 ppm). Actually the change of the coordination mode of vacataporphyrin to palladium determined for $[(VPH_2\text{-}4)Pd^{II}]^+$ can be readily appreciated by analysis of coordination shifts defined here as a ^{13}C chemical shift difference between the $(VPH_2\text{-}1)Pd^{II}Cl$ and $[(VPH_2\text{-}4)Pd^{II}]^+$ at chosen positions. These values equal C(1) 10.8, C(2) 37.9, C(7) 5.6, C(8) −2.4, C(12) 5.0 ppm and clearly point out C(2) and C(3) acting as a coordinating unit.[69–75]

The degeneracy of $[(VPH_2\text{-}4)Pd^{II}]^+$ resonances is removed for $[(VPHMe\text{-}4)Pd^{II}]^+$. Thus three pyrrolic AB patterns have been detected even though they are in the similar region as determined for $[(VPH_2\text{-}4)Pd^{II}]^+$ (5.0−6.0 ppm). The atypical ^{1}H chemical shift values resemble those of $[(VPH_2\text{-}4)Pd^{II}]^+$. The peculiar downfield position of the H(3) resonance (8.04 ppm) has been preserved but the effect is evidently smaller as compared to the nonmethylated counterpart.

The ^{1}H NMR spectrum of $[(VPH_2\text{-}4)Pd^{II}]^+$ complies with the C_2 molecular symmetry. The twisted structure of $[(VPH_2\text{-}4)Pd^{II}]^+$(Scheme 3) accounts for the presence of the paratropic effect. Such a macrocyclic conformation affords the palladium η^2-C(2)C(3) interaction. The C(2) and C(3) atoms are located at the opposite sides of the N_3 plane owing to the perpendicular orientation of the C(2)C(3) bond. Actually the C(2)C(3) fragment acquires the common orientation of the η^2-alkene for

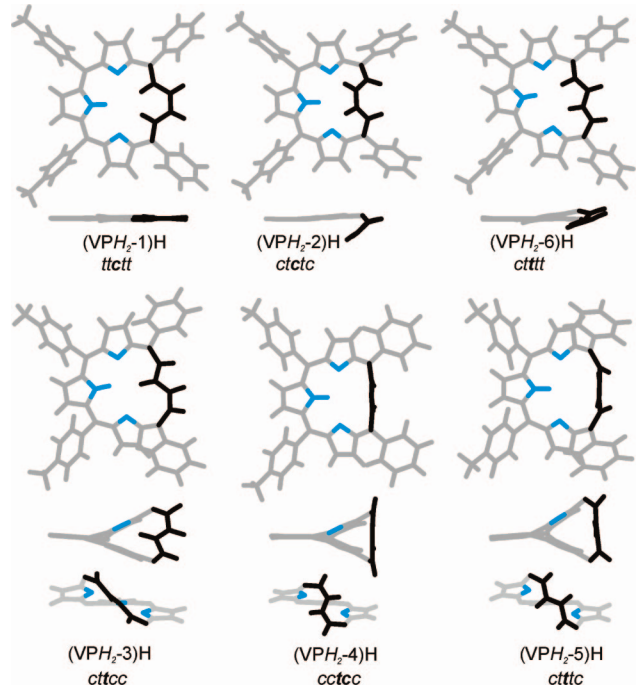

Figure 8. Geometries of vacataporphyrin stereoisomers $(VPH_2\text{-}n)H$ obtained in a DFT optimization for level B3LYP/6-31G**. Projections emphasize the conformations of macrocycle. The configuration of C(20)C(1)C(2)C(3)-C(4)C(5) is described as in the text.

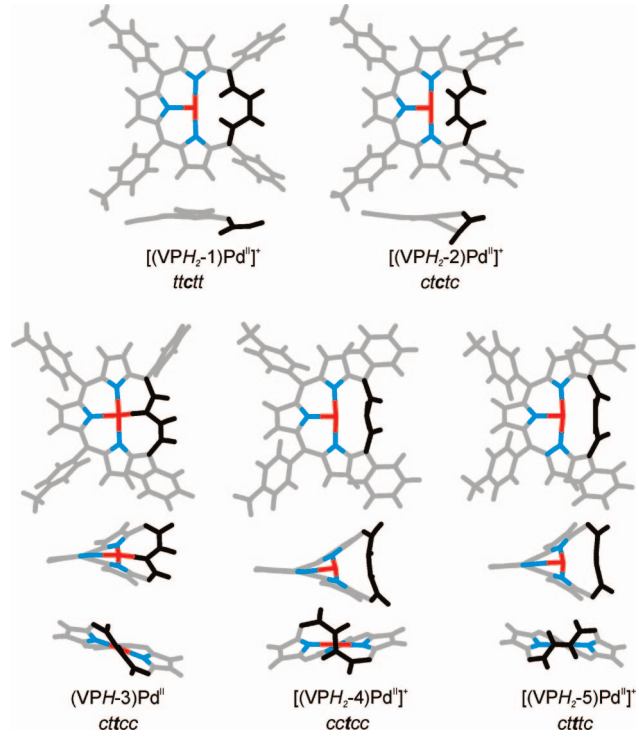

Figure 9. Geometries of palladium vacataporphyrin complexes obtained in a DFT optimization for level B3LYP/LANL2D. Projections emphasize the conformations of the macrocycle. The configuration of C(20)C(1)C(2)-C(3)C(4)C(5) is described as in the text.

the square planar palladium complexes containing the −C≡C− moiety.[70] For instance, a similar coordination geometry, involving chelate rings, was reported for a cyclometallated hydridoosmium complex of a phosphine-based pincer ligand.[76] There the η^2-alkene moiety is encompassed in the pincer ligand (*E*)-

(69) Elschenbroich, C.; Salzer, A. *Organometallics-A concise Introduction*; VCH: Weinheim, Germany, 1989.
(70) Hahn, C.; Vitagliano, A.; Giordano, F.; Taube, F. *Organometallics* **1998**, 2960–2066.
(71) Bernard, G. M.; Wasylishen, R. E.; Phillips, A. D. *J. Phys. Chem.* **2000**, *104*, 8131–8141.
(72) Hahn, C.; Morvillo, P.; Vitagliano, A. *Eur. J. Inorg. Chem.* **2001**, 419–429.
(73) Hahn, C.; Morvillo, P.; Herdtweck, E.; Vitagliano, A. *Organometallics* **2002**, *21*, 1807–1818.
(74) Cavallo, L.; Macchioni, A.; Zucaccia, C.; Zuccaccia, D.; Orabona, I.; Ruffo, F. *Organometallics* **2004**, *23*, 2137–2145.
(75) Ghebreyessus, K. Y.; Ellern, A.; Angelici, R. J. *Organometallics* **2005**, *24*, 1725–1736.

$Ph_2P(CH_2)_2CH{=}CH(CH_2)_2PPh_2$ allowing the meridional coordination via two phosphine and η^2-{CH=CH} centers. Similarly the chiral palladium(0) complexes with 15-membered triolefinic macrocyclic ligands present the comparable coordination geometry consistent with the trans stereochemistry in the palladacyclopropane rings.[77]

One has to notice that a fundamental chain of transformations, (VPH_2-1)Pd^{II}Cl → (VPH-3)Pd^{II} → [(VPH_2-4)Pd^{II}]$^+$ (Schemes 2 and 3), requires a series of profound conformational rearrangements. Primarily the structural changes involve the C(20)-C(1)C(2)C(3)C(4)C(5) annulene fragment. For the sake of convenience a conformation with respect to each bond is symbolically described as t (trans) or c (cis) respectively. Thus this sequence of reactions is associated with the following conformational changes [ttctt] → [cc**t**tc] → [cc**t**cc]. Here it is important to recall that the AA′XX′ pattern of H(1), H(2), H(3), and H(4) resonances of (VPH_2-1)Pd^{II}Cl presents the NMR parameters which resemble those of [18]annulene.[20,21] In particular $^3J_{12}$ = 12.6 Hz and $^3J_{23}$ = 9.8 Hz coupling constants are consistent with trans and cis arrangement of the respective hydrogens. In noticeable contrast the AA′XX′ pattern (H(1)-H(2)H(3)H(4)) of [(VPH_2-4)Pd^{II}]$^+$ gives a markedly different set of coupling constants: $^3J_{12}$ = 5.8 Hz and $^3J_{23}$ = 14.9 Hz. These values are, however, consistent with a trans arrangement of H(2), H(3) hydrogens and are diagnostic of the S-like skeleton which is unique for the [(VPH_2-4)Pd^{II}]$^+$ structure.[78] The structural models, generated by DFT calculations (vide infra), have been used to visualize the suggested structures of [(VPH_2-4)Pd^{II}]$^+$ and [(VP*HME*-4)Pd^{II}]$^+$ (Figures 6 and 9) and to evaluate the degree of the porphyrin distortion and the proximity of hydrogens.

All spectroscopic evidence indicated that the [(VPH_2-4)Pd^{II}]$^+$ complex has C_2 symmetry and contains an S-like C(20)C(1)C(2)-C(3)C(4)C(5) structural motif. [(VP*HME*-4)Pd^{II}]$^+$ preserves the identical structural feature, albeit the molecular symmetry due to the substitution is lowered. Concurrently the structural analysis has been carried out using NOE. The relay of observed and assigned NOE connectivities for [(VP*HME*-4)Pd^{II}]$^+$ is presented in Figure 6. The analytically decisive set of the NOE effects, unique for the S-like geometry, results from through-space interactions: 2-CH_3···H(7) (a) and 2-CH_3···5-*o*-Ph (b).

Alternative Route to [(VPH_2-4)Pd^{II}]$^+$. The addition of $AgBF_4$ to the solution of (VPH_2-1)Pd^{II}Cl in $CDCl_3$ results in formation of the complex cations [(VPH_2-1)Pd^{II}(PhCN)]$^+$ or [(VPH_2-1)Pd^{II}(H_2O)]$^+$. Traces of benzonitrile (introduced in the course of insertion) or water are sufficient to introduce respective ligands to the coordination sphere. The methathesis reaction, carried out in dark, has been followed by ^{1}H NMR spectroscopy. The spectroscopic patterns of [(VPH_2-1)Pd^{II}(PhCN)]$^+$ or [(VPH_2-1)Pd^{II}(H_2O)]$^+$ (Figure 7, trace A) resemble maternal (VPH_2-1)Pd^{II}Cl (Figure 2). Characteristically, the upfield relocated resonances of coordinated benzonitrile have been readily identified at 6.19, 6.97, and 7.19 ppm for *o*-H, *m*-H and *p*-H, respectively (298 K, $CDCl_3$). The resonance of the coordinated water molecule has been detected at −1.17 ppm (250 K). It has also been found that [(VPH_2-1)Pd^{II}(PhCN)]$^+$ remains stable

Scheme 4. Alternative Route of Conversion of (VPH_2-1)Pd^{II}Cl into [(VPH_2-4)Pd^{II}]$^+$

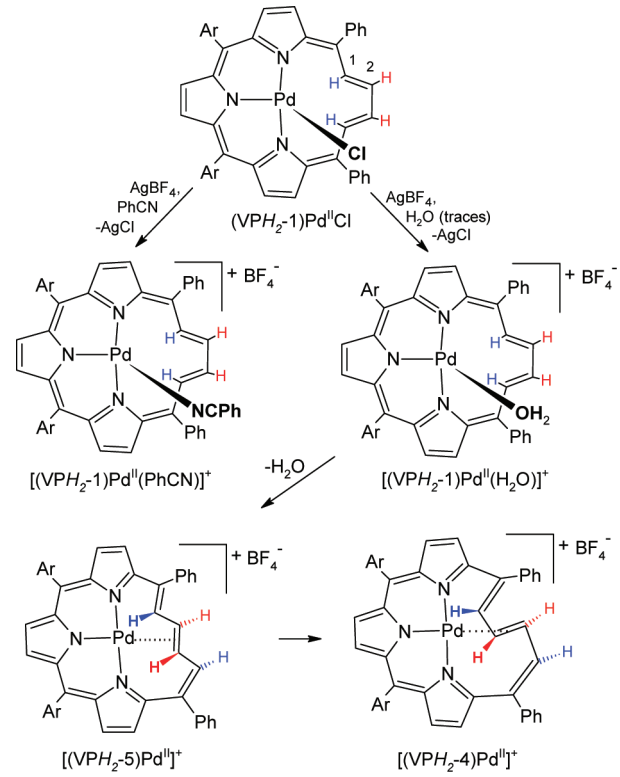

in solution once protected from light. In contrast, the [(VPH_2-1)Pd^{II}(H_2O)]$^+$ species is unstable at 298 K as data in Figure 7 show. Evidently the fourth coordination position becomes available to be occupied by C(2)C(3) moiety after a removal of weakly bound water. In trace A (Figure 7) one can see the spectrum of [(VPH_2-1)Pd^{II}(H_2O)]$^+$ at 250 K. In standing at 298 K for 150 seconds the peaks due to the starting species decrease in intensity as shown in trace B (the spectrum measured at 250 K to prevent the further transformation). As [(VPH_2-1)Pd^{II}-(H_2O)]$^+$ decomposes an unstable intermediate, [(VPH_2-5)Pd^{II}]$^+$, forms which eventually decays after 4 h (298 K) into independently identified (see above) [(VPH_2-4)Pd^{II}]$^+$ being the sole stable product of the reaction (Scheme 4). The time of decay (298 K) of [(VPH_2-5)Pd^{II}]$^+$ can be hastened to a few minutes by the presence of light. At applied conditions the transformation of [(VPH_2-5)Pd^{II}]$^+$ into [(VPH_2-4)Pd^{II}]$^+$ is irreversible.

The ^{1}H NMR spectrum of [(VPH_2-5)Pd^{II}]$^+$ (Figure 7B) resembles the basic features of [(VPH_2-4)Pd^{II}]$^+$ (Figures 7C and 5B, discussed for the 10,15-bis(4-methoxyphenyl) derivatives) consistent with residual Möbius antiaromaticity, albeit the effect is markedly less pronounced ([(VPH_2-5)Pd^{II}]$^+$: $\delta_{H(2)}-\delta_{H(1)}$ = 1.63 ppm, [(VPH_2-4)Pd]$^+$: $\delta_{H(2)}-\delta_{H(1)}$= 2.67 ppm). The ^{1}H NMR spectrum of [(VPH_2-5)Pd^{II}]$^+$ (250 K) exhibits one AB (6.77, 6.35 ppm) and one A_2 (6.47 ppm) patterns assigned to pyrrole resonances. The reversed order of meso-phenyl resonances has been observed (*p*-H > *m*-H > *o*-H). In particular the upfield relocation of the ortho protons (7.30 ppm) seems to be of significance. The remote position of the methine H(2) resonance at 7.67 ppm has also been noted. The AA′XX′ pattern assigned to H(1), H(2), H(3), and H(4) of [(VPH_2-5)Pd^{II}]$^+$ gives the following coupling constants: $^3J_{12}$ = 6.4 Hz and $^3J_{23}$ = 10.2 Hz, which suggests the strongly twisted conformation of the butadiene part.[78] One has to realize that deceptively similar spectra of [(VPH_2-5)Pd^{II}]$^+$ and (VPH_2-2)Zn^{II}Cl[19] demonstrate

(76) Liu, S. H.; Huang, X.; Lin, Z.; Lau, C. P.; Jia, G. *Eur. J. Inorg. Chem.* **2002**, 1697–1702.
(77) Pla-Quintana, A.; Roglans, A.; de Julián-Ortiz, J. V.; Moreno-Mañas, M.; Parella, T.; Benet-Buchholz, J.; Solans, X. *Chem. Eur. J.* **2005**, *11*, 2689–2697.
(78) Gernel, C.; Mereiter, K.; Schmid, R.; Kirchner, K. *Organometallics* **1997**, *16*, 2623–2626.

Scheme 5. Transformations of Palladium Vacataporphyrin (Transient Species in Braces)

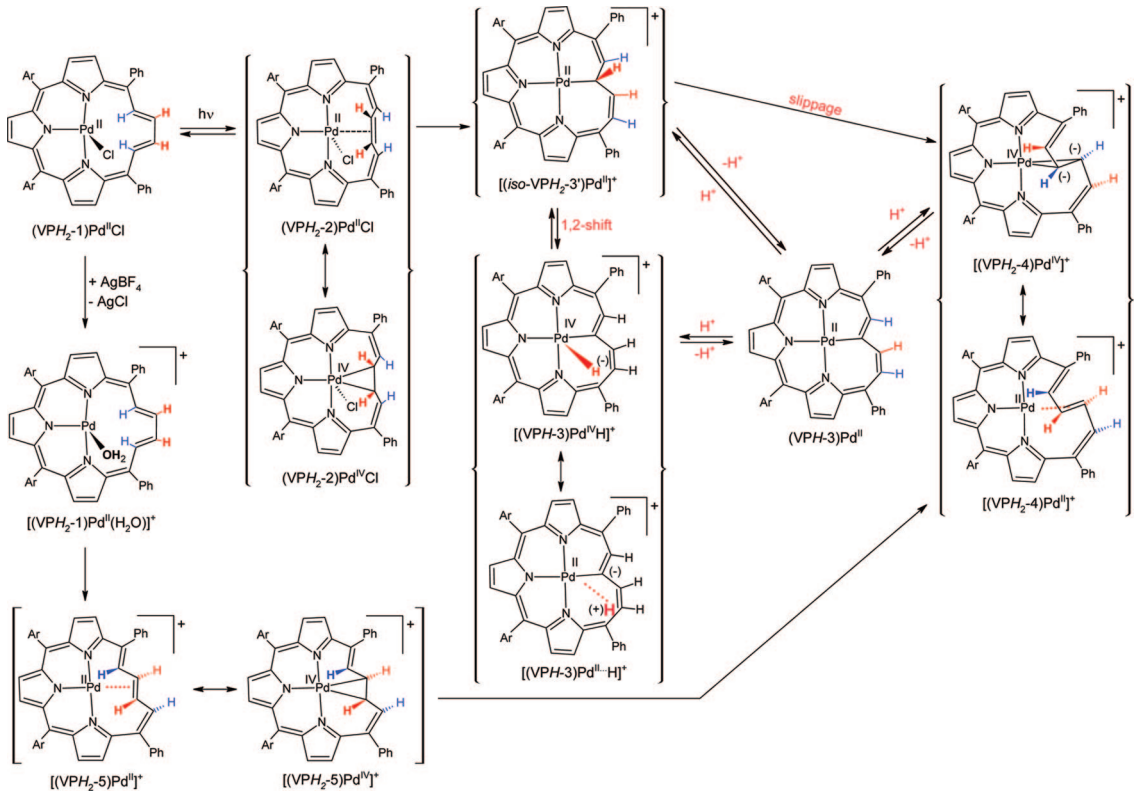

the reversed position of H(1) and H(2) resonances as accounted by differences in the macrocyclic conformation.

Reaction Mechanisms. The formation of (VP*H*-3)Pd^{II} from (VPH_2-1)Pd^{II}Cl or [(VPH_2-4)Pd^{II}]$^+$can be considered as a special case of C−H activation assisted by intramolecular palladium coordination. Actually such a process can be classified as a classical cyclometalation but being confined into a macrocyclic cavity. Several examples of such chemistry have been elaborated in the pincer ligand environment.[79–81] In fact the formation of palladium(II) carbaporphyrinoids[16,23–26,28,29,82–84] or palladium(II) hexaphyrin[85] provides the appropriate examples as well.

The first step (Scheme 5) is conformational rearrangement [(VPH_2-1)Pd^{II}]$^+$ ⇄ {[(VPH_2-2)Pd^{II}]$^+$} (from now on acronyms of transient species are given in braces), affording the η^2-interaction in {[(VPH_2-2)Pd^{II}]$^+$ ↔ [(VPH_2-2)Pd^{IV}]$^+$}. Subsequently an electrophilic process may produce a transient palladium(II) complex of *iso*-vacataporphyrin {[(*iso*-VPH_2-3′)Pd^{II}]$^+$} affording a σ-coordination of tetrahedral C(2) carbon atom, where *iso*-vacataporphyrin (*iso*-VPH_3), is a hypothetical tautomer of vacataporphyrin formed by relocation of NH hydrogen on the C(2) atom. In the case of relevant pincer ligands an arenium form is involved in the analogous transient stage.[79–81,86–90] The following dissociation of H$^+$ from {[(*iso*-VPH_2-3′)Pd^{II}]$^+$} yields (VP*H*-3)Pd^{II}. An alternative route involves a 1,2-shift affording the hydridopalladium(IV) complex {[(VP*H*-3)Pd^{IV}H]$^+$}. The reductive elimination eventually produces (VP*H*-3)Pd^{II}. Importantly the replacement of strongly bound chloride in (VPH_2-1)Pd^{II}Cl by relatively weakly bound water triggered an independent route to form [(VPH_2-4)Pd^{II}]$^+$ which involves a new intermediate [(VPH_2-5)Pd^{II}]$^+$ but omits the (VP*H*-3)Pd^{II} species.

The mechanism suggested for methylation of (VP*H*-3)Pd^{II} is presented in Scheme 6. An initial oxidative addition of MeI in the presence of $AgBF_4$ may afford a methylpalladium(IV) species {[(VP*H*-3)Pd^{IV}Me]$^+$}.[91] This step should be followed by a 1,2-shift from palladium(II) to the C(2) carbon yielding the palladium(II) complex of 2-Me-*iso*-vacataporphyrin {[(*iso*-VP*HMe*-3′)Pd^{II}]$^+$} where the tetrahedral C(2) carbon atom binds palladium(II). The next transformation seems to be unique to a macrocyclic environment as the methylation product is forced to remain in the adjacency of palladium(II). The appropriately prearranged structure of {[(*iso*-VP*HMe*-3′)Pd^{II}]$^+$} undergoes a smooth slippage to afford the η^2-complex [(VP*HMe*-4)Pd^{II}]$^+$.

(79) Canty, A. J.; van Koten, G. *Acc. Chem. Res.* **1995**, *28*, 406–413.
(80) Albrecht, M.; van Koten, G. *Angew. Chem., Int. Ed.* **2001**, *40*, 3750–3781.
(81) van der Boom, M. E.; Milstein, D. *Chem. Rev.* **2003**, *103*, 1759–1792.
(82) Graham, S. R.; Ferrence, G. M.; Lash, T. D. *Chem. Commun.* **2002**, 894–895.
(83) Liu, D.; Ferrence, G. M.; Lash, T. D. *J. Org. Chem.* **2004**, *69*, 6079–6093.
(84) Furuta, H.; Kubo, N.; Maeda, H.; Ishizuka, T.; Osuka, A.; Nanami, H.; Ogawa, T. *Inorg. Chem.* **2000**, *39*, 5424–5425.
(85) Mori, S.; Shimizu, S.; Taniguchi, R.; Osuka, A. *Inorg. Chem.* **2005**, *44*, 4127–4129.
(86) Grove, D. M.; van Koten, G.; Louwen, J. N.; Noltes, J. G.; Spek, A. L.; Ubbels, H. J. *J. Am. Chem. Soc.* **1982**, *104*, 6609–6616.
(87) Terheijden, J.; van Koten, G.; Vinke, I. C.; Spek, A. L. *J. Am. Chem. Soc.* **1985**, *107*, 2891–2898.
(88) Albrecht, M.; Dani, P.; Lutz, M.; Spek, A. L.; van Koten, G. *J. Am. Chem. Soc.* **2000**, *122*, 11822–11833.
(89) Albrecht, M.; Spek, A. L.; van Koten, G. *J. Am. Chem. Soc.* **2001**, *123*, 7233–7246.
(90) Vigalok, A.; Milstein, D. *Acc. Chem. Res.* **2001**, *34*, 798–807.
(91) DFT optimizations demonstrated that the putative methylpalladium IV) [(VP*H*-3)Pd^{IV}Me]$^+$ is highly unstable relatively to [(VP*HMe*-4)Pd^{II}]$^+$ as the respective energy difference equals 38.40 kcal/mol. Thus [((VP*H*-3)Pd^{IV}Me]$^+$ may play at best a role of a transient species (see Tables S14, S15 of the Supporting Information).

Scheme 6. Mechanism of Alkylation

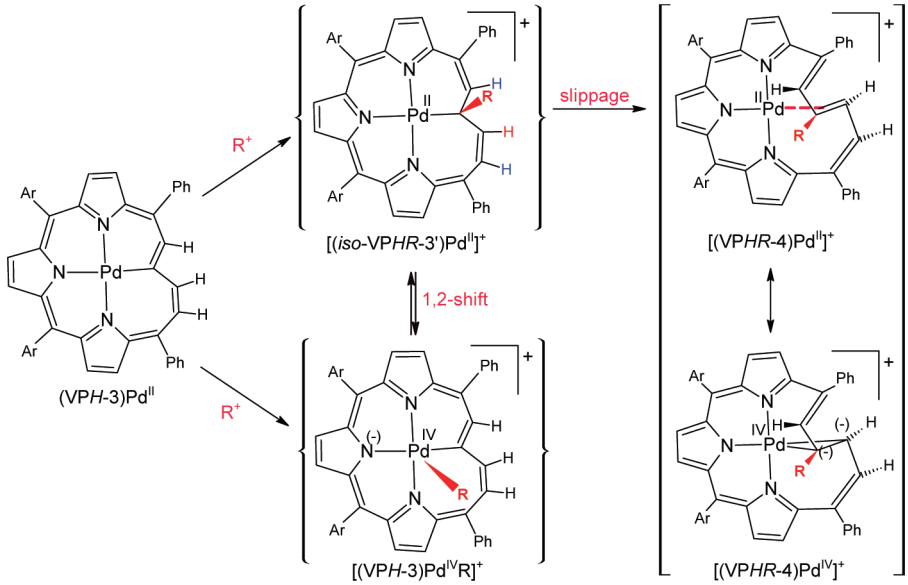

A protonation of (VP*H*-3)Pd^{II} will follow the identical sequence of reactions forming eventually [(VPH_2-4)Pd^{II}]$^+$ (Scheme 5). Contrary to methylation, the protonation is reversible (Scheme 3). The conversion from [(VPH_2-4)Pd^{II}]$^+$ to (VP*H*-3)Pd^{II} includes a rearrangement to {[(*iso*-VPH_2-3′)Pd^{II}]$^+$} followed by dissociation. An alternative path of the transformation (VP*H*-3)Pd^{II} → [(VPH_2-4)Pd^{II}]$^+$ involves a direct protonation or methylation of (VP*H*-3)Pd^{II} at the activated C(2) carbon.

DFT Calculations: Vacataporphyrin. Density functional theory (DFT) has been successfully used to describe the properties of porphyrins and related systems, providing information on their conformational behavior, tautomerism, and aromaticity.[92] We have previously applied DFT modeling to study the relationship between aromaticity, tautomerism, and coordinating capabilities of carbaporphyrinoids.[23,42,43,93–96] In particular, we demonstrated the energetic preference of a free vacataporphyrin for a nearly planar conformation.[1,19] In direct analogy to an unorthodox geometry of 21,23-ditelluraporphyrin,[40] the inverted geometry of the free ligand was considered. The hypothetical inverted geometry of vacataporphyrin has been trapped by coordination of nickel(II), zinc(II), or cadmium(II) ions.[19]

Specific coordination constraints of palladium(II) may promote a variety of plausible macrocyclic conformations in accordance with the fascinating conformational flexibility of an annulene moiety. Consequently we have considered several novel geometries of vacataporphyrin being evidently inspired by the experimentally determined ligand structures supported by palladium coordination. These conformers were subjected to a DFT optimization at the B3LYP/6-31G** level of theory.

Table 1. Selected Calculated Geometrical Parameters, Relative Energies, and Nucleus-Independent Chemical Shift (NICS) for Vacataporphyrin Conformers

	(VPH_2-1)H	(VPH_2-2)H	(VPH_2-3)H	(VPH_2-4)H	(VPH_2-5)H	(VPH_2-6)H
E^a	0	7.02	8.05	19.68	14.05	8.18
$NICS_{B3LYP}{}^b$	−13.6	−7.5	−7.7	+6.0	+4.0	−1.7
$NICS_{KMLYP}{}^c$	−12.6	−3.9	−2.0	+4.4	+4.6	−9.1
C(20)−C(1)^d	1.384	1.377	1.373	1.471	1.357	1.391
C(1)−C(2)^d	1.405	1.426	1.432	1.351	1.457	1.402
C(2)−C(3)^d	1.398	1.369	1.366	1.453	1.348	1.385
C(3)−C(4)^d	1.405	1.426	1.435	1.351	1.457	1.399
C(4)−C(5)^d	1.384	1.377	1.369	1.471	1.357	1.439
standard deviation^e	0.011	0.028	0.035	0.063	0.057	0.021

[a] *E* relative to (VPH_2-1)H, kcal/mol, calculated using the B3LYP/6-31G**//B3LYP/6-31G** approach. [b] NICS in ppm, calculated by GIAO-B3LYP method for B3LYP/6-31G** geometries. [c] NICS in ppm, calculated by GIAO-B3LYP method for KMLYP/6-31G** geometries. [d] In Å, for B3LYP/6-31G** geometries. [e] Bond length standard deviation along the C(20)C(1)C(2)C(3)C(4)C(5) annulene fragment.

The final B3LYP geometries are shown in Figure 8. To present a complete picture, the previously optimized structures (VPH_2-1)H and (VPH_2-2)H are included.

A genuine energy minimum was obtained for all structures. The calculated total energies, using the B3LYP/6-31G**//B3LYP/6-31G** approach (Table 1) demonstrate that the planar conformer is the most stable, which accounts for the preference for (VPH_2-1)H in the solution and in the solid state. The relative energy of conformers increases in a series (VPH_2-1)H < (VPH_2-2)H < (VPH_2-3)H ≤ (VPH_2-6)H < (VPH_2-5)H < (VPH_2-4)H. Actually these values are relatively low. An analysis of the calculated relative stabilities of conformers provides some additional insight into the coordinating properties of vacataporphyrin. Previously, considering the mechanism of metal ion insertion into the coordination core of inverted porphyrin or 2-oxybenziporphyrin we included a preorganization step into the mechanistic route.[23,97] Thus, to satisfy the requirements imposed by the inserted metal ion the molecular and electronic structures of the ligand have to be prearranged. Such a step may contribute to an overall activation energy of metal insertion.

(92) Ghosh, A. Quantum Chemical Studies of Molecular Strucutres and Potential Energy Surafaces of Porphyrins and Hemes. In *The Porphyrin Handbook*; Kadish, K. M., Smith, K. M., Guilard, R., Eds.; Academic Press: San Diego, CA, 2000; pp 1−38.
(93) Stępień, M.; Latos-Grażyński, L.; Szterenberg, L. *J. Org. Chem.* **2007**, *72*, 2259–2270.
(94) Myśliborski, R.; Latos-Grażyński, L.; Szterenberg, L.; Lis, T. *Angew. Chem., Int. Ed.* **2006**, *45*, 3670–3674.
(95) Pawlicki, M.; Latos-Grażyński, L.; Szterenberg, L. *Inorg. Chem.* **2005**, *44*, 9779–9786.
(96) Pawlicki, M.; Latos-Grażyński, L.; Szterenberg, L. *J. Org. Chem.* **2002**, *67*, 5644–5653.
(97) Szterenberg, L.; Latos-Grażyński, L. *Inorg. Chem.* **1997**, *36*, 6287–6291.

Table 2. Selected Calculated (B3LYP/LANL2DZ) Geometrical Parameters and Relative Energies for Palladium Complexes of Vacataporphyrin

	$[(VPH_2\text{-}1)Pd^{II}]^+$	$[(VPH_2\text{-}2)Pd^{II}]^+$	$(VPH\text{-}3)Pd^{II}$	$[(VPH_2\text{-}4)Pd^{II}]^+$	$[(VPH_2\text{-}5)Pd^{II}]^+$
E^a	15.12	5.96		0	6.21
Pd−C(1)[b]	3.229	3.336	3.024	3.137	3.188
Pd−C(2)[b]	4.136	2.480	2.025	2.290	2.431
Pd−C(3)[b]	4.136	2.481	3.105	2.277	2.431
Pd···H(1)[b]	2.450	4.130	3.991	4.046	3.957
Pd···H(2)[b]	5.100	2.656		2.772	2.800
C(20)−C(1)[b]	1.391	1.370	1.385	1.373	1.367
C(1)−C(2)[b]	1.418	1.449	1.448	1.468	1.467
C(2)−C(3)[b]	1.400	1.391	1.403	1.414	1.385
C(3)−C(4)[b]	1.418	1.449	1.420	1.467	1.465
C(4)−C(5)[b]	1.391	1.370	1.388	1.373	1.367
angle $C_{butad}\backslash N_3$[c]	4.5	46.3	30.9	90.1	90.0
standard deviation[d]	0.014	0.040	0.026	0.047	0.051

[a] *E* relative to $[(VPH_2\text{-}4)Pd]^+$, kcal/mol, calculated using the B3LYP/LANL2DZ//B3LYP/LANL2DZ approach. [b] In Å. [c] In deg. [d] Bond length standard deviation along the C(20)C(1)C(2)C(3)C(4)C(5) annulene fragment.

Energies of a direct preorganization evaluated for $(VPH_2\text{-}1)H \rightarrow (VPH_2\text{-}n)H$ ($n > 1$), are equal to the relative energy of the conformers (Table 1). These values are comparable with activation energies determined for metal ion insertion to porphyrins and *N*-methylporphyrins.[98–101] Alternatively a stepwise conversion can be considered as a route facilitating conformational transformations of $(VPH_2\text{-}1)H$ into any given conformer. For instance the most energetically demanding transformation $(VPH_2\text{-}1)H \rightarrow (VPH_2\text{-}4)H$ can be realized in sequence $(VPH_2\text{-}1)H$ [tt**c**tt] → $(VPH_2\text{-}5)H$ [ct**t**tc] → $(VPH_2\text{-}4)H$ [cc**t**cc] where the energy difference for each subsequent step is below 15 kcal/mol. The relatively small calculated ligand preorganization energy explains why vacataporphyrin coordinates acquiring several different macrocyclic conformations.

DFT Calculations: Palladium Vacataporphyrin. The experimentally observed conformers of palladium vacataporphyrin raised the question of their relative stability. To approach this problem we have applied the density functional theory (DFT) in the similar way as previously described for metallocarbaporphyrinoids and zinc(II) and cadmium(II) vacataporphyrin.[19,23,42,43,95,102] The principal geometries of palladium(II) vacataporphyrin complexes have been already schematically presented above in Schemes 3 and 5. The appropriate structures were subjected to a DFT optimization at the B3LYP/LANL2DZ level of theory. The final geometries corresponding to $[(VPH_2\text{-}1)Pd^{II}]^+$, $[(VPH_2\text{-}2)Pd^{II}]^+$, $(VPH\text{-}3)Pd^{II}$, $[(VPH_2\text{-}4)Pd^{II}]^+$, and $[(VPH_2\text{-}5)Pd^{II}]^+$ are shown in Figure 9. In each case a genuine energy minimum was obtained (B3LYP/LANL2DZ). Selected geometrical parameters and relative energies are given in Table 2.

The energy ordering of $[(VPH_2)Pd^{II}]^+$ stereoisomers is $[(VPH_2\text{-}4)Pd^{II}]^+ < [(VPH_2\text{-}2)Pd^{II}]^+ \leq [(VPH_2\text{-}5)Pd^{II}]^+ < [(VPH_2\text{-}1)Pd^{II}]^+$. Most importantly the experimentally detected sequence of reactions results eventually in the most stable molecular state. Unexpectedly, the strongly folded macrocyclic structure of vacataporphyrin provides energetically the most favorable condition for palladium(II) coordination. Here it is important to realize that the computational results correspond to cationic molecules where one coordination site is readily accessible once chloride of $(VPH_2\text{-}1)Pd^{II}Cl$ has been removed. The direct energy comparison excludes $(VPH\text{-}3)Pd^{II}$ which is formally a product of the proton dissociation from $[(VPH_2\text{-}1)Pd^{II}]^+$ or $[(VPH_2\text{-}4)Pd^{II}]^+$.

The interaction involving the palladium(II) and the butadiene fragment in $[(VPH_2\text{-}2)Pd^{II}]^+$, $[(VPH_2\text{-}4)Pd^{II}]^+$, and $[(VPH_2\text{-}5)Pd^{II}]^+$ is of special interest. The dihedral angle between the butadiene plane and the plane of the three pyrrolic nitrogens (C_4/N_3) at the hypothetical $[(VPH_2\text{-}2)Pd^{II}]^+$ is similar as found from DFT optimized structures of zinc(II) or cadmium(II) vacataporphyrins.[19] The interaction, as quantified by the distances M···H, M···C (Table 2), is indeed affected by the conformational changes under study. For instance, in the $[(VPH_2\text{-}2)Pd^{II}]^+$ conformer, the separation between palladium and C(2) or C(3) (2.481 Å) is smaller than the expected van der Waals contact (ca. 3.3 Å)[103] but still larger than normally observed Pd−C bond lengths as the typical values for Pd^{II}−C(η^2-alkene) complexes are in the order of 2.18 Å,[104,105] although the longer bond distance have been reported as well (e.g., Pd(II)−C, 2.273(7) Å;[70] Pd(I)−C, 2.388(3)−2.495(4)[106]). The projection of the palladium(II) ion onto the C(1)C(2)C(3)C(4) plane (C_4 plane) lies close to the center of the C(2)−C(3) bond, so the metal ion interacts in an η^2 fashion although in peculiar position of the ethylene fragment with respect of the nearly coplanar molecular fragment containing tripyrrolic unit and palladium(II). The conformer $[(VPH_2\text{-}5)Pd^{II}]^+$ reveals a weak η^2 interaction, with Pd−C(2) and Pd−C(3) distances being equal at 2.431 Å.[70,105] The zigzag shape of C(20)C(1)C(2)C(3)C(4)C(5) orients the central C(2)C(3) fragment coplanarly with the PdN_3 plane filling the fourth corner of the square-planar structure. Eventually the conformational transformation afforded $[(VPH_2\text{-}4)Pd^{II}]^+$, allowing η^2 interactions where the Pd−C(2) and Pd−C(3) distances equal 2.290 and 2.277 Å, respectively. These distances are still longer than the upper limits of the regular palladium(II)−carbon bond.[70,105] The S-like shape of C(20)-C(1)C(2)C(3)C(4)C(5) orients the central C(2)C(3) bond per-

(98) Bain-Ackerman, M. J.; Lavallee, D. K. *Inorg. Chem.* **1979**, *18*, 3358–3364.
(99) Hambright, P.; Chock, P. B. *J. Am. Chem. Soc.* **1974**, *96*, 3123–3131.
(100) Longo, R. F.; Brown, E. M.; Quimby, D. J.; Adler, A. D.; Meot-Ner, M. *Ann. N.Y. Acad. Sci.* **1973**, *206*, 420–442.
(101) Longo, R. F.; Brown, E. M.; Rau, G. W.; Adler, A. D. In *The Porphyrins*; Dolphin, D., Ed.; Academic Press: New York, 1978; p 459−481.
(102) Chmielewski, M. J.; Pawlicki, M.; Sprutta, N.; Szterenberg, L.; Latos-Grażyński, L. *Inorg. Chem.* **2006**, *45*, 8664–8671.
(103) Bondi, A. *J. Phys. Chem.* **1964**, *68*, 441–451.
(104) Binotti, B.; Bellachioma, G.; Cardaci, G.; Macchion, A.; Zuccaccia, C.; Foresti, E.; Sabatino, P. *Organometallic* **2006**, *21*, 346–354.
(105) Orpen, A. G.; Brammer, L.; Allen, F. H.; Kennard, O.; Watson, D. G. *J. Chem. Soc., Dalton Trans.* **1989**, S1–S83.
(106) Dotta, P.; Kumar, P. G. A.; Pregosin, P. S. *Organometallics* **2004**, *23*, 4247–4254.

Scheme 7. Building Blocks of Vacataporphyrin[a]

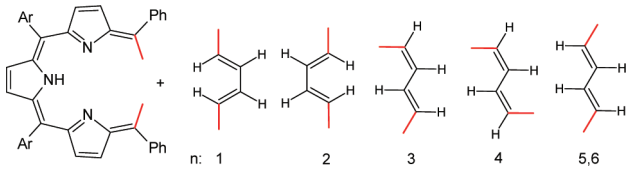

[a] The *n* identifies the conformer of (VPH_2-*n*)H; locations of linkage are in red.

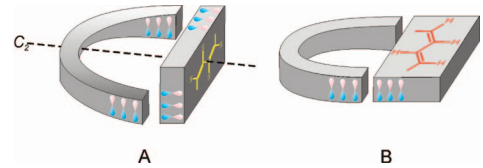

Figure 10. Strategy to construct (A) Möbius and (B) Hückel conformers of vacataporphyrin.

pendicularly to the PdN_3 plane completing the fourth corner of the square-planar structure. The vector of the C(2)−C(3) bond is nearly orthogonal to the coordination plane, bisected by it. Thus the first coordination spheres of [(VPH_2-4)Pd^{II}]$^+$ and [(VPH_2-5)Pd^{II}]$^+$ resemble d^8 palladium complexes containing the ethylene ligand.[70,72]

Hückel and Möbius Macrocyclic Topologies. In the conformational analysis of vacataporphyrin and its complexes it is significant to notice that molecule combines two fundamental building blocks: a tripyrrin with terminal C(5) and C(20) meso carbon atoms and a butadiene fragment in its compact (*s*-cis) or extended (*s*-trans) conformations shown in Scheme 7. These two fundamental conformations of butadiene can be accommodated by tripyrrin and eventually preserved in the resulting structure acquiring suitable macrocyclic conformations.

The tripyrrin part has to adjust its geometry to constraints imposed by butadiene. The planar geometry of tripyrrin is preserved in (VPH_2-1)H, (VPH_2-2)H, and (VPH_2-6)H where the *s-cis*-butadiene (first two) or *s-trans*-butadiene (the last) unit can be readily identified. To join the tripyrrin fragment and *s-trans*-butadiene moiety to get an architecture of (VPH_2-3)H, (VPH_2-4)H, or (VPH_2-5)H, the terminal carbon atoms C(5) and C(20) have to occupy positions above and below the plane defined by the N(23) and two adjacent meso carbon atoms. This adjustment imposes a pronounced helical twist creating a nonplanar structure of tripyrrin which resembles helical conformations identified for a number of metallobiliverdins[107,108] and a palladium tripyrrin complex.[109] The extent of the twist is readily reflected by an improper torsion angle C(5)−C(10)−C(15)−C(20). These corresponding values equal (VPH_2-1)H, 3.1°; (VPH_2-2)H, 0.1°; (VPH_2-3)H, 42.6°; (VPH_2-4)H, 42.8°; (VPH_2-5)H, 55.4°; (VPH_2-6)H, 11.5°. Due to the marked helicity of the tripyrrin chain the conformers (VPH_2-3)H, (VPH_2-4)H, (VPH_2-5)H are chiral. Thus in Figures 8 and 9 only single enantiomers have been shown.

Herges and co-workers in their inspiring contribution on synthesis of the first Möbius annulenes[54,55] noticed that these molecules exhibit two types of conjugation: (1) "normal" conjugation with p orbitals perpendicular to the ring plane and sp^2 carbon atoms in their preferred trigonal planar configuration and (2) in-plane conjugation with pyramidalized carbon atoms. Their successful synthetic strategy involved a connection of a pyramidalized building block that is kept in its strained configuration by a rigid molecular frame and a regular π system. In our analysis we have noticed that the two structural motives of vacataporphyrin may introduce "normal" (tripyrrin) and in-plane (*s-trans*-butadiene) conjugations once comprised in a single molecular structure (Figure 10, trace A). The *s-trans*-butadiene moiety is perpendicular to the C_2 axis of tripyrrin. Consequently the Möbius structure can be achieved by combining normal and in-plane conjugation. One can readily notice that an alternative mode of tripyrrin and butadiene connections (both fragments are located in parallel planes) creates a molecule acquiring the Hückel topology (Figure 10, trace B).

In more general terms, conjugated cyclic molecules can be classified as Hückel or Möbius systems, depending on the number of half-twists in the ring. The molecules with an even number of half-twists are predicted to follow the Hückel rule, whereas those with an odd number of half-twists (Möbius systems) follow the reverse Hückel rule.[47] Alternatively, the topology can be determined by counting the number of trans bonds along the [18]annulenoid conjugation pathway.[50] Significantly, the Hückel rule is reversed and 4*n*-electron Möbius annulenes are aromatic whereas the (4*n* + 2)-electron systems are antiaromatic.[44,46,47]

In the case of vacataporphyrin or its palladium complexes the distinction between Möbius and Hückel topology is facilitated by the fact that despite the differences in helicity of tripyrrin moiety these fragments conserve an even number of half-twists for any (VPH_2-*n*)H conformer. Consequently the straightforward structural analysis focuses solely on C(20)C(1)C(2)C(3)C(4)C(5). As inferred from our considerations (VPH_2-1)H, [tt**c**tt]; (VPH_2-2)H, [ct**c**tc]; (VPH_2-3)H [ct**t**cc]; (VPH_2-6)H [tt**t**tc] have the Hückel topology. Notably (VPH_2-4)H [cc**t**cc] and (VPH_2-5)H [ct**t**tc] acquire the Möbius topology. Evidently the most stable stereoisomer of a free vacataporphyrin belongs to the familiar group of Hückel annulenes.[47,110] The evidently large energy differences between the most stable Hückel (VPH_2-1)H and other conformers rule out their contribution to any conformational equilibria.

The coordination of palladium preserves the fundamental structural features of free base vacataporphyrin including the extent of the tripyrrin twist defined as above [(VPH_2-1)Pd^{II}]$^+$, 0.0°; [(VPH_2-2)Pd^{II}]$^+$, 0.5°; (VP*H*-3)Pd^{II}, 45.2°; [(VPH_2-4)Pd^{II}]$^+$, 51.7°; [(VPH_2-5)Pd^{II}]$^+$, 57.9°. Importantly [(VPH_2-4)Pd^{II}]$^+$ and [(VPH_2-5)Pd^{II}]$^+$ conformers have Möbius topology where the remaining palladium complexes are described by Hückel topology. Significantly the torsional angles along the macrocyclic skeleton of [(VPH_2-4)Pd^{II}]$^+$ vary in the range 0°−42.8° (176.3−151.6°) which is in the limit 0°−50° (180°−130°) required for the efficient π conjugation in the Möbius band.[44] Predictably[44,48,111,112] the stronger alternations of bond lengths have been found for antiaromatic molecules with Möbius topology in comparison to aromatic Hückel ones

(107) Balch, A. L.; Mazzanti, M.; Noll, B. C.; Olmstead, M. M. *J. Am. Chem. Soc.* **1994**, *116*, 9114–9122.
(108) Nguyen, K. T.; Rath, S. P.; Latos-Grażyński, L.; Olmstead, M. M.; Balch, A. L. *J. Am. Chem. Soc.* **2004**, *126*, 6210–6211.
(109) Bröring, M.; Brandt, C. B. *J. Chem. Soc., Dalton Trans.* **2002**, 1391–1395.
(110) Rzepa, H. S. *Org. Lett.* **2005**, *7*, 4637–4639.
(111) Pohl, M.; Schmickler, H.; Lex, J.; Vogel, E. *Angew. Chem., Int. Ed. Engl.* **1991**, *30*, 1693–1697.
(112) Cissel, J. A.; Vaid, T. P.; Yap, G. P. A. *Org. Lett.* **2006**, *8*, 2401–2404.

(Tables 1, 2) as reflected by larger values of mean standard deviations of bond lengths along the C(20)C(1)C(2)C(3)C(4)C(5) route.

Significantly the stability order is reversed in comparison to the free base vacataporphyrin (Tables 1 and 2). In contrast to vacataporphyrin conformers the Möbius structure [(VPH_2-4)Pd^{II}]$^+$ can be considered as a fundamental state for the whole series. Thus the coordination of palladium(II) imposes additional structural constrains on vacataporphyrin and affords the remarkable stabilization of Möbius geometries, for example, [(VPH_2-4)Pd^{II}]$^+$ (0) versus [(VPH_2-1)Pd^{II}]$^+$ (15.12 kcal/mol). The most importantly two Möbius [(VPH_2-5)Pd^{II}]$^+$ and [(VPH_2-4)Pd^{II}]$^+$ conformers have been **experimentally** identified. Despite the obvious energetic preferences for the Möbius form [(VPH_2-4)Pd^{II}]$^+$ as determined by DFT optimization, two Hückel conformers (VPH_2-1)Pd^{II}Cl and (VP*H*-3)Pd^{II} have been detected as well. Their stabilization results from coordination of chloride to yield (VPH_2-1)Pd^{II}Cl or from formation of the Pd−C bond as seen for (VP*H*-3)Pd^{II}.

Chemical Shifts and NICS Calculations. Nucleus-independent chemical shifts (NICS) have been proposed by Schleyer et al. as a computational measure of aromaticity that is related to experimental magnetic criteria.[113,114] A NICS is defined as the negative shielding value computed at the center of a ring. The NICS method has been used to assess the aromaticity of annulenes or porphyrins[115,116] and their analogues.[93,117] NICS values were calculated using GIAO-B3LYP method for (VPH_2-*n*)H molecules for the central 17-membered ring (Table 1). Comparison of the center ring NICS (calculated for B3LYP/6-31G** geometries) values shows that they are good indicators of macrocyclic aromaticity. For the Hückel aromatic systems (VPH_2-1)H and (VPH_2-3)H the central NICS values are negative (−13.6 and −7.7 ppm, respectively) and comparable with that reported for a porphyrin (−16.5 ppm).[115] For the Möbius antiaromatic conformers (VPH_2-4)H and (VPH_2-5)H the center ring NICS are positive (+6.0 and +4.0 ppm, respectively). These values are smaller than the NICS obtained for [20]annulene (+12.1 ppm)[48] but similar to values determined previously for antiaromatic tautomer of 22-hydroxybenziporphyrin (+5.0 ppm).[93]

The NICS calculations (by the same, GIAO-B3LYP method) have been also done using KMLYP/6-31G** geometries (Table 1 and Supporting Information, Table S2) to limit an overestimation of π contribution. Using these geometries, the NICS values for (VPH_2-4)H and (VPH_2-5)H equal +4.4 and +4.6, respectively. Thus they are comparable to those found for B3LYP/6-31G** geometries (+6.0 and +4.0). Evidently they are consistent with the Möbius antiaromaticity resulting from the Möbius topology of these crucial structures. The NICS values calculated for KMLYP/6-31G** optimized Hückel structures (VPH_2-1)H, (VPH_2-2)H, (VPH_2-3)H, and (VPH_2-6)H reflect their aromatic nature although these values are notably less negative than found for B3LYP/6-31G** geometries (Table 1).

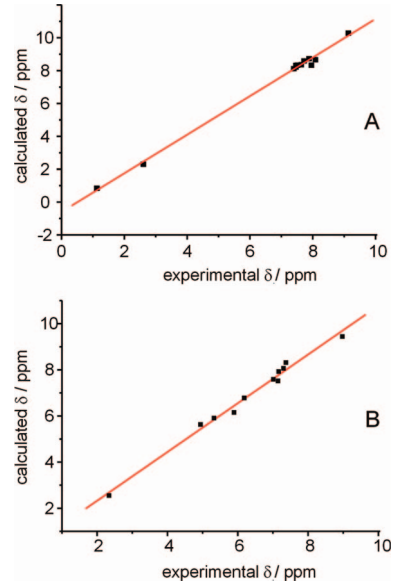

Figure 11. Linear correlation between calculated (GIAO-B3LYP//B3LYP/6-31G**) and experimental values of chemical shifts for the representative Hückel and Möbius conformers (A) (VPH_2-1)Pd^{II}Cl (B) [(VPH_2-4)Pd^{II}]$^+$.

^{1}H NMR chemical shifts have been calculated using the GIAO-B3LYP method for the B3LYP/LANL2DZ geometries of [(VPH_2-*n*)Pd^{II}]$^+$ and (VPH_2-1)Pd^{II}Cl which acquire Hückel or Möbius macrocyclic topologies (Figure 11 and Figure S1). The presence of a paratropic ring current is a commonly accepted indicator of antiaromatic character.[118,119] Paratropicity causes shielding of the protons located on the outside of the ring and deshielding, often substantial, of the protons inside the ring. The paratropic ring current is thus a reversal of the more common diatropic current associated with aromaticity which yields the deshielding of the perimeter protons and the substantial shielding of the internal ones. It is significant to make a point that the Hückel conformers of vacataporphyrin are aromatic but the Möbius conformer systems are antiaromatic as discussed above. The paratropicity is expected to generate an upfield relocation of β-H resonances and the reversed order of meso-aryl resonances (*meso*-phenyl, *p*-H > *m*-H > *o*-H; *meso*-*p*-tolyl, *m*-H > *o*-H). The analysis of the calculated chemical shifts reveals that indeed the chemical shift pattern reflects quantitatively the features predicted for Hückel or Möbius topologies of [(VPH_2-*n*)Pd^{II}]$^+$ listed above.

In the case of the described palladium vacataporphyrin complexes we have been in a unique position to compare the experimental and calculated chemical shifts assigned to Hückel and Möbius geometries. We have concluded that there is a satisfactory qualitative agreement for each considered set of theoretical and experimental data readily demonstrated by linear correlations between the calculated and experimental chemical shifts shown for two representative examples of Hückel [(VPH_2-1)Pd^{II}]Cl (aromatic) or Möbius [(VPH_2-4)Pd^{II}]$^+$ (antiaromatic) topologies (Figure 11). Still the calculated paratropicity or diatropicity are overestimated. For instance in the case of Möbius topology the differences in calculated (B3LYP) and experimental ^{1}H NMR shifts reach maximally 0.9 ppm. The visible differences have been detected for indisputably aromatic (VPH_2-1)PdCl (max 1.1 ppm for H(2,3)). This effect is likely

(113) Schleyer, P. v. R.; Meaerker, C.; Dransfeld, A.; Jiao, H.; Hommes, N. J. R. v. E. *J. Am. Chem. Soc.* **1996**, *118*, 6317–6318.
(114) Chen, Z.; Wannere, C. S.; Corminboeuf, C.; Puchta, R.; Schleyer, P. v. R. *Chem. Rev.* **2005**, *105*, 3842–3888.
(115) Cyrański, M. K.; Krygowski, T. M.; Wisiorowski, M.; Hommes, N. J. R. v. E.; Schleyer, P. v. R. *Angew. Chem., Int. Ed. Engl.* **1998**, *37*, 177–180.
(116) Jusélius, J.; Sundholm, D. *J. Org. Chem.* **2000**, *65*, 5233–5237.
(117) Furuta, H.; Maeda, H.; Osuka, A. *J. Org. Chem.* **2001**, *66*, 8563–8572.
(118) Pople, J. A.; Untch, K. G. *J. Am. Chem. Soc.* **1966**, *88*, 4811–4815.
(119) Lazzeretti, P. *Phys. Chem. Chem. Phys.* **2004**, *6*, 217–223.

due to the known propensity of the B3LYP functional to overestimate π-conjugation.[120] The calculated chemical shifts of hypothetical $[(VPH_2\text{-}2)Pd^{II}]^+$ resemble those found for appropriate conformer of $(VPH_2\text{-}2)Zn^{II}Cl$ or $(VPH_2\text{-}2)Cd^{II}Cl$ complexes.[19]

Conclusions

Vacataporphyrin can be described as an annulene-porphyrin hybrid. The macrocycle contains the relatively rigid tripyrrin moiety which affords the limited flexibility resembling regular porphyrins. In contrast the butadiene fragment can readily adopt several conformations consistent with the annulene-like nature of vacataporphyrin. Thus the combination of both structural components allows a unique flexibility of the whole conjugated macrocycle albeit constrained by tripyrrin fragment and eventually by coordination. In this contribution we have demonstrated that vacataporphyrin acts as ligand to palladium which is firmly held via three pyrrolic nitrogen atoms. Two fundamental ways of interactions between palladium and annulene fragment have been recognized. The first one resemble an η^2-type interaction and involves a C(2)C(3) unit of the butadiene part. The second one imposed the profound conformational changes allowed to create the regular Pd−C bond demonstrating that vacataporphyrin acts as "true" carbaporphyrinoid.

Vacataporphyrin, applied as a ligand toward palladium(II) and previously to zinc(II) and cadmium(II), reveals the peculiar plasticity of its molecular and electronic structure. This important feature has enabled us to investigate and eventually to control the subtle interplay between their structural flexibility and aromaticity. In particular the coordinated vacataporphyrin may acquire the relatively planar Hückel or extremely rare twisted Möbius topologies which are reflected by aromatic or antiaromatic properties of 18-electron π-system, respectively. The properties of specific conformers were studied using ^{1}H NMR and supported by DFT calculations. Actually we have experimentally identified the very first example of Möbius antiaromaticity. Thus vacataporphyrin provides a stimulating environment to investigate coordination chemistry of the Möbius-type macrocyclic ligand. Efforts to explore such coordination chemistry are underway.

Experimental Section

Solvents and Reagents. Dichloromethane-d_2 (CIL) was used as received. Chloroform-d (CIL) was passed through basic Al_2O_3. Vacataporphyrin (VPH_2-*1*)H derivatives (5,20-diphenyl-10,15-di(*p*-tolyl)-21-vacataporphyrin, 10,15-bis(4-metoxyphenyl)-5,20-diphenyl-21-vacataporphyrin, and their deuterated analogues) have been obtained according to the previously described procedures.[1,19]

(VPH_2-1)PdCl. A 6.5 mg (0.010 mmol) portion of (VPH_2-1)H, was dissolved in 15 mL of $CHCl_3$ with 5 μL of triethylamine. Nitrogen was bubbled through the solution for 20 min. The flask was carefully protected from light with black paper. Subsequently 6.8 mg (0.018 mmol) of $Pd(PhCN)_2Cl_2$ was added. The mixture was stirred at room temperature for 20 min. The progress of the reaction was checked by UV−vis spectroscopy, and if necessary another portions of $Pd(PhCN)_2Cl_2$ and triethylamine were added. The resulting mixture was evaporated to dryness with a vacuum rotary evaporator (the flask was always wrapped in the black paper). Typically the insertion is quantitative. Recrystallization was performed from CH_2Cl_2 and CH_3OH. If the product was contaminated with (VPH-3)Pd^{II}, it was chromatographed in dark on a short silica gel 40 column with CH_2Cl_2 (second, green fraction).

Data for (VPH_2-1)Pd^{II}, Ar = *p*-Tol. UV−vis, CH_2Cl_2 $\lambda(\log\varepsilon)$: 394 (4.5), 442 (4.7), 616 (sh), 663 (4.3). ^{1}H NMR: δ 9.14 (AA′XX′, $^3J_{1,2} = 12.6$ Hz, $^3J_{2,3} = 9.8$ Hz, $^4J_{1,3} = -1.5$ Hz, 2H, 2,3), 8.09 (*d*, $J = 4.6$ Hz, 2H, 8,17), 7.99 (*s*, 2H, 12,13), 7.96 (*d*, $J = 4.6$ Hz, 2H, 7,18), 7.89 (*d*, $J = 7.7$ Hz, 2H, *o*-Tol), 7.73 (*d*, $J = 7.1$ Hz, 4H, *o*-Ph), 7.64 (*d*, $J = 7.7$ Hz, 2H, *o*-Tol), 7.52 (*t*, $J = 7.1$ Hz, 4H, *m*-Ph), 7.47 (*m*, 4H, *p*-Ph, *m*-Tol), 7.40 (*d*, $J = 7.7$ Hz, 2H, *m*-Tol), 2.61 (*s*, 6H, *p*-Tol-CH_3), 1.13 (AA′XX′, 2H, 1,4). ^{13}C NMR: δ 165.7 (6,19), 142.3 (11,14), 140.8 (9,16), 138.6 (*ipso*-Ph), 138.2 (*p*-Tol), 138.0 (2,3), 136.9 (*ipso*-Tol), 136.8 (5,20), 136.1 (1,4), 133.9 (8,17), 133.1 (*o*-Tol), 132.7 (10,15), 132.5 (*o*-Ph), 132.1 (*o*-Tol), 130.8 (7,18), 130.5 (12,13), 128.2 (*m*-Ph), 127.9, and 127.8 (*m*-Tol, *p*-Ph), 127.7 (*m*-Tol), 21.5 (CH_3-Tol). HRMS (EI, *m*/*z*): 734.1801 (734.1782 for $C_{46}H_{34}N_3{}^{106}Pd^+$).

(VPH-3)Pd^{II}. A solution of (VPH_2-1)PdCl (10 mg, 0.016 mmol) in dichloromethane (50 mL) was stirred in the daylight for 1 day. The solution was concentrated to 1−2 mL and chromatographed on a short silica gel or alumina grade III column. The first, green fraction eluted with CH_2Cl_2 contained the desired product. The solvent was evaporated, the green solid (VPH-3)Pd^{II} was dried in vacuum. Yield 80%.

Data for (VPH_2-3)Pd^{II}Cl, Ar = *p*-Tol. UV−vis, CH_2Cl_2 $\lambda(\log\varepsilon)$: 345 (4.4), 376 (4.4), 428 (sh), 461 (5.0), 542 (3.7), 600 (sh), 653 (4.3). ^{1}H NMR: δ 9.75 (dd, $^4J_{1,3} = 0.9$ Hz, $^3J_{3,4} = 9.2$ Hz, 1H, 3), 8.96 (d, $^4J_{1,3} = 0.9$ Hz, 1H, 1), 8.25 (d, $^3J = 4.7$ Hz, 1H, 13), 8.08 (d, $^3J = 9.2$ Hz,1H, 4), 8.02 (d,$^3J = 5.0$ Hz,1H, 8), 7.89 (*d*, 2H, 20-*o*-Ph), 7.89 (*s*, 2H, 17, 18), 7.87 (*d*,$^3J = 5.0$ Hz, 1H, 12), 7.76 (*d*, $^3J = 4.7$ Hz, 1H, 7), 7.72 (*d*, $^3J = 7.5$ Hz, 2H, 15-*o*-Tol), 7.66 (*d*, $^3J = 7.3$ Hz, 2H, 10-*o*-Tol), 7.59 (*t*,$^3J = 7.5$ Hz, 2H, 20-*m*-Ph), 7.54 (*d*, $^3J = 7.3$ Hz, 2H, 5-*o*-Ph), 7.50 (*t*,$^3J = 7.3$ Hz, 1H, 20-*p*-Ph), 7.44 (*t*, $^3J = 7.1$ Hz, 2H, 5-*m*-Ph), 7.40 (m, 3H, 15-*m*-Tol, 5-*p*-Ph), 7.35 (*d*, $^3J = 8.0$ Hz, 2H, 10-*m*-Tol), 2.57 (*s*, 3H, 15-*p*-Tol (CH_3)), 2.54 (*s*, 3H, 10-*p*-Tol (CH_3)). ^{13}C NMR: δ 155.5, 151.7, 151.0, 145.1, 143.5, 142.3, 142.0, 141.1, 139.9, 139.2, 138.0, 137.8, 137.7, 137.3, 136.7 136.0, 135.3, 133.6, 132.7, 132.6, 132.4, 132.2, 131.8, 131.7, 131.3, 131.0, 129.5, 128.3, 128.2, 127.9, 127.8, 127.6, 127.4, 127.3, 127.1, 122.0, 21.40 21.41. HRMS (EI, *m*/*z*): 733.1734 (733.1704 for $C_{46}H_{33}N_3{}^{106}Pd^+$).

[(VPH_2-4)Pd^{II}]BF_4. A 5 equiv portion of HBF_4 (diethyl ether solution) was added to the (VPH-3)Pd^{II} solution in CH_2Cl_2. The green solution turns immediately brown. The solvents were evaporated, and the brown solid, pure [(VPH_2-4)Pd^{II}]BF_4, was dried in vacuum.

Data for [(VPH_2-4)Pd^{II}]BF_4, Ar = *p*-Tol. UV−vis, CH_2Cl_2 $\lambda(\log\varepsilon)$: 376 (sh), 423 (4.6), 525 (sh). ^{1}H NMR: δ 8.98 (AA′XX′, $^3J_{1,2} = 5.8$ Hz, $^3J_{2,3} = 14.9$ Hz, $^4J_{1,3} = -1.3$ Hz, $^5J_{1,4} = 1.1$ Hz 2H, 2,3), 7.37 (t, $^3J = 7.5$ Hz, 2H, *p*-Ph), 7.30 (t, $^3J = 7.6$ Hz, 4H, *m*-Ph), 7.15 (m, 8H, *o*-Ph, *m*-Tol), 7.01 (br. d, $^3J = 7.2$ Hz, 4H, *o*-Tol) 6.18 (AA′XX′, 2H, 1,4), 5.89 (d, $^3J = 4.9$ Hz, 2H, 8,17), 5.33 (d, $^3J = 4.9$ Hz, 2H, 7,18), 4.95 (s, 2H, 12,13), 2.36 (s, 6H, *p*-Tol-CH_3); ^{13}C NMR: δ 136.3 (8,17), 129.8 (*p*-Ph), 128.6 (*m*-Ph), 128.6 (*m*-Tol), 128.4 (*o*-Tol), 127.4 (*o*-Ph), 125.5 (12,13), 125.3 (1,4), 125.2 (7,18), 100.1 (2,3), 21.5 (*p*-Tol-CH_3). HRMS (ESI, *m*/*z*): 734.1801 (734.1782 for $C_{46}H_{34}N_3{}^{106}Pd^+$).

^{1}H NMR Data for [(VPH_2-4)Pd^{II}]BF_4, Ar = Anis. δ 8.91 (AA′XX′, $^3J_{1,2} = 5.8$ Hz, $^3J_{2,3} = 14.9$ Hz, $^4J_{1,3} = -1.3$ Hz, $^5J_{1,4} = 1.1$ Hz, 2H, 2,3), 7.36 (t, $^3J = 7.4$ Hz, 2H, *p*-Ph), 7.29 (t, $^3J = 7.7$ Hz, 4H, *m*-Ph), 7.18 (d,$^3J = 7.3$ Hz, 4H, *o*-Ph), 7.10 (d, $^3J = 8.4$ Hz, 4H, *o*-Anis), 6.87 (d,$^3J = 8.7$ Hz, 4H, *m*-Anis), 6.24 (AA′XX′, 2H, 1,4), 5.98 (d, $^3J = 4.9$ Hz, 2H, 8,17), 5.37 (d, $^3J = 4.9$ Hz, 2H, 7,18), 5.01 (s, 2H, 12,13), 3.83 (s, 6H, OCH_3).

[(VPH_2-5)Pd^{II}]BF_4. An NMR sample of (VPH_2-1)PdCl in $CDCl_3$ was treated in dark with excess of $AgBF_4$ and shaked for a few minutes. The product was not isolated. The degree of conversion was up to 90%. The solution of [(VPH_2-5)Pd^{II}]BF_4 is very unstable in light, moderately stable in the dark (298 K). All the 2D NMR spectra were obtained in low temperature. The full description was not possible because of the gradual conversion into [(VPH_2-4)Pd^{II}]BF_4.

(120) Wannere, C. S.; Sattelmeyer, K. W.; Schaefer, H. F., III; Schleyer, P. v. R. *Angew. Chem., Int. Ed.* **2004**, *43*, 4200–4206.

Data for [(VPH$_2$-5)Pd^{II}]BF$_4$, Ar = Anis. UV−vis, CH_2Cl_2 $\lambda(\log\varepsilon)$: 404 (4.3), 444 (4.3), 616 (3.8), 815 (4.0). ^{1}H NMR (250 K): δ 7.67 (AA′XX′, $^3J_{1,2}$ = 6.4 Hz, $^3J_{2,3}$ = 10.2 Hz, $^4J_{1,3}$ = −1.4 Hz, 2H, 2,3), 7.41 (m, 6H, *m,p*-Ph), 7.35 (d, 4H, *o*-Anis), 7.31 (d, 4H, *o*-Ph), 6.99 (d, ^3J = 8.8 Hz, 4H, *m*-Anis), 6.77 (d, ^3J = 4.9 Hz, 2H, 8,17), 6.47 (s, 2H, 12,13), 6.35 (d, ^3J = 4.9 Hz, 2H, 7,18), 6.04 (AA′XX′, 2H, 1,4), 3.89 (s, 6H, OCH_3). ^{13}C NMR: δ 142.2 (1,4), 140.4 (8,17), 133.1 (*o*-Anis), 130.6 (*m*-Ph), 130.4 (12,13), 129.8 (*p*-Ph), 129.3 (*o*-Ph), 125.8 (7,18), 120.8 (2,3), 114.0 (*m*-Anis).

[(VP*HMe*-4)Pd^{II}]BF$_4$. A toluene solution of (VP*H*-3)Pd^{II} (3 mg, 0.005 mmol) was heated under nitrogen. Twenty-five μL of methyl iodide (0.40 mmol) was added and the solution was refluxed for 3 min. Then 20 mg of $AgBF_4$(0.10 mmol) was added. AgI precipitated immediately and the solution turned slowly brown. After 5 more minutes of boiling, the mixture was filtered through glass wool and the solution was dried. Typically the insertion is quantitative and does not require any further purification.

Data for [(VP*HMe*-4)Pd^{II}]BF$_4$, Ar = Anis. UV−vis, CH_2Cl_2 λ ($\log\varepsilon$): 379 (sh), 430 (4.7). ^{1}H NMR, (CD_2Cl_2)**:** δ 8.04 (d, ^3J = 6 (5.7 Hz) Hz, 1H, 3), 7.67 (d, ^3J = 8.0 Hz, 1H, *o*-Ph), 7.62 (t, ^3J = 7.8 Hz, 1H, *p*-Ph), 7.48 (t, 2H, *m*-Ph), 7.41 (m, 6H, Ar), 7.22 (d, ^3J = 8.1 Hz, 2H, 5-*o*-Ph), 7.14 (m, 5H, *m*-Anis, Ph), 6.90 (2d, ^3J = 8.8 Hz, 4H, *o*-Anis), 6.34 (d, ^3J = 4.8 Hz, 1H, 17) 6.25 (d, ^3J = 4.8 Hz, 1H, 8), 6.11 (d, ^3J = 5.7 Hz, 1H, 4), 5.67 (s, 1H, 1), 5.61 (d, ^3J = 4.8 Hz, 1H, 18), 5.54 (d, ^3J = 4.8 Hz, 1H, 7), 5.31 (d, ^3J = 4.5 Hz, 1H, 12), 5.24 (d, ^3J = 4.5 Hz, 1H, 13), 3.81 (s, 6H, OCH_3), 3.17 (s, 3H, 2-CH_3). ^{13}C NMR: δ 136.8 (17), 136.8 (8), 132.2 (*m*-Ph), 130.6 (*m*-Anis), 129.6 (Ph), 128.8 (o-Ph), 128.4 (Ph), 127.4 (1), 127.3 (Ph), 126.8 (Ph), 126.0 (12), 125.2 (18), 125.0 (13), 123.1 (7), 120.9 (4), 113.5 (*o*-Anis), 91.8 (3), 55.1 (OCH_3), 24.5 (2-CH_3). HRMS (ESI, *m*/*z*): 780.1852 (780.1859 for $C_{47}H_{36}N_3O_2{}^{106}Pd^+$).

(VP*CH*$_3$-3)Pd^{II}. [(VP*HMe*-4)Pd^{II}]BF_4 (3 mg) was dissolved in a methanol solution of Et_4NCl (25 mg) and stirred for 30 min at 50 °C. The solvent was evaporated and the solid was dissolved in 1 mL of CH_2Cl_2 and filtered through a short column of Al_2O_3 grade III. Yield ca. 60%.

Data for (VP*Me*-3)Pd^{II}, Ar = Anis. UV−vis, CH_2Cl_2 $\lambda(\log\varepsilon)$: 351 (4.5), 381 (4.5), 465 (4.9), 669 (4.4). ^{1}H NMR: δ (CD_2Cl_2) 8.46 (s, 1H, 1), 8.06 (d, ^3J = 4.8 Hz, 1H, 17), 7.77 (d, ^3J = 4.9 Hz, 1H, 8) 7.75 (d, ^3J = 7.3 Hz, 2H, 20-*o*-Ph), 7.68 (d, ^3J = 8.4 Hz, 2H, 15-*o*-Anis), 7.64 (d, ^3J = 8.8 Hz, 2H, 10-*o*-Anis), 7.62 (d, ^3J = 4.3 Hz, 1H, 12), 7.59 (d, ^3J = 4.5 Hz, 1H, 13), 7.58 (d, ^3J = 4.7 Hz, 1H, 18), 7.51 (t, ^3J = 7.7 Hz, 2H, 20-*m*-Ph), 7.46 (m, 4H, 7, 20-*p*-Ph, 5-*o*-Ph), 7.39 (m, 4H, 5-*m,p*-Ph), 7.40 (s, 4), 7.11 (d, ^3J = 8.8 Hz, 2H, 15-*m*-Anis), 7.07 (d, ^3J = 8.8 Hz, 2H, 10-*m*-Anis), 3.93 (s, 3H, 15-*p*-OCH_3), 3.91 (s, 3H, 10-*p*-OCH_3), 3.41 (s, 3H, 2-CH_3). ^{13}C NMR: δ 159.6, 159.4, 154.8, 153.8, 144.1, 143.2, 142.7, 141.0, 140.8, 140.7, 139.5, 137.3, 135.5, 134.8, 134.8, 134.4, 133.4, 133.2, 132.9, 131.4, 131.0, 131.0, 130.5, 130.2, 129.0, 128.5, 127.9, 127.5, 127.1, 127.0, 125.5, 112.3, 112.2. HRMS (ESI, *m*/*z*): 780.1821 (780.1859 for $C_{47}H_{35}N_3O_2{}^{106}Pd + H^+$).

Instrumentation. NMR spectra were recorded on a highfield spectrometer (frequencies: ^{1}H 500.13 MHz, ^{13}C 125.77 MHz) equipped with either a broadband inverse gradient probehead or a direct broadband probehead. Absorption spectra were recorded on a diode array spectrometer. High resolution mass spectra were recorded on spectrometers using the electrospray and electron impact techniques.

X-Ray Analysis. X-ray quality crystals (VPH_2-1)PdCl·CH_2Cl_2 were prepared by diffusion of methanol into dichloromethane solution contained in a thin tube stored in the refrigerator. Data were collected at 100 K on Kuma KM4CCD diffractometer using Cu Kα radiation (λ = 1.54180 Å). The data were corrected for Lorentz and polarization effects. An analytical absorption correction was applied. Crystal data are compiled in the CIF file in the Supporting Information. The structure was solved using direct methods with SHELXS-97 and refined against F^2 using SHELXL-97 (G. M. Sheldrick, University of Göttingen, Germany, 1997) with anisotropic thermal parameters for the non-hydrogen atoms. Scattering factors were those incorporated in SHELXS-97.[121,122]

Theoretical Calculations. DFT calculations were performed with the Gaussian 03 program.[123] Geometry optimizations were carried out within unconstrained C_1 symmetry. Starting geometries were obtained using molecular mechanics and semiempirical calculations.

B3LYP[124,125] and KMLYP[126,127] hybridization of the exchange funtional DFT were used with the LANL2DZ basis set for metal complexes and 6-31G** for the free ligands.[128] The structures were found to have converged to a minimum on the potential energy surface; the resulting zero-point vibrational energies were included in the calculation of relative energies. NICS values were calculated at the GIAO-B3LYP/6-31G** level for the optimized structures. Calculations of NMR properties for investigated systems were performed for the optimized structures.

Acknowledgment. Financial support from the Ministry of Science and Higher Education (Grant PBZ-KBN-118/T09/2004) is kindly acknowledged. Quantum chemical calculations have been carried out at the Poznań Supercomputer Center (Wrocław).

Supporting Information Available: Complete ref 123; tables of computational results (Cartesian coordinates); figures presenting correlations between calculated and experimental ^{1}H NMR chemical shifts for (VP*H*-3)Pd^{II}, [(VPH_2-5)Pd^{II}]$^+$, [(VPH_2-1)Pd^{II}]$^+$, and [(VPH_2-4)Pd^{II}]$^+$; tables of selected calculated (with KMLYP functional) geometrical parameters for [(VPH_2-1)Pd^{II}]$^+$, [(VPH_2-4)Pd^{II}]$^+$, and (VPH_2-*n*)H; crystallographic data in CIF format for (VPH_2-1)PdCl. This material is available free of charge via the Internet at http://pubs.acs.org.

JA711039C

(121) Sheldrick, G. M. *SHELXS97: Program for Crystal Structure Solution;* University of Göttingen: Göttingen, Germany, 1997.
(122) Sheldrick, G. M. *SHELXL97: Program for Crystal Structure Refinement;* University of Göttingen: Göttingen, Germany, 1997.
(123) Frisch, M. J., et al. *Gaussian 03,* revision C.01; Pittsburgh, PA, 2004.
(124) Becke, A. D. *Phys. Rev. A* **1988**, *38*, 3098–3100.
(125) Lee, C.; Yang, W.; Parr, R. G. *Phys. Rev. B* **1988**, *37*, 785–789.
(126) Kang, J. K.; Musgrave, C. B. *J. Chem. Phys.* **2001**, *115*, 11040–11051.
(127) Senosiain, J. P.; Han, J. H.; Musgrave, C. B.; Golden, D. M. *Faraday Discuss.* **2002**, *119*, 173–189.
(128) Hay, P. J.; Wadt, W. R. *J. Chem. Phys.* **1985**, *82*, 270–283; 284−298; 299−310.